Spatiotemporal Marginal-Cost-Based Retail Electricity Markets: Efficiency, Structure and Feasibility

Elli Ntakou, *Student Member, IEEE*
Division of Systems Engineering, Boston University
entakou@bu.edu

Michael Caramanis, *Senior Member, IEEE*
Division of Systems Engineering, Boston University
mcaraman@bu.edu

Abstract— We [1] address the extension of spatiotemporal marginal-cost-based Wholesale Transmission markets to Retail Distribution markets. Key challenges include (i) a broader range of significant cost components and requirements such as real and reactive power marginal losses, transformer life degradation, and voltage control, (ii) higher order of magnitude of retail market participants, some with complex needs and capabilities such as flexible loads (e.g. EVs, HVAC with inter-temporal consumption utility) and distributed generators and resources (e.g. power electronics whose excess capacity can provide reactive power compensation and voltage control), and (iii) the need to model inherently non-convex AC load flow relationships to represent the aforementioned costs and requirements. To this end, we define the detailed distribution market clearing problem and solve it to derive real and reactive power Distribution Location-Marginal-Prices (DLMPs). Using industrial and commercial/residential distribution feeders adapted from real Southern California Edison data we derive day-ahead market solutions for several scenarios and use the associated 24 hour DLMP trajectories to discuss the broader efficiency and sustainability impact of dynamic distribution/retail markets.

Keywords:distribution network locational marginal prices; power flow; reactive power compensation; voltage control; distributed generation; dual use of power electronics; transformer loss of life; distribution network rent

I. INTRODUCTION

Following a long discussion in the literature launched by Vickrey's seminal work on dynamic pricing of utility services [1] and its detailed application to Electric Power [2, 3], short- term marginal-cost-based Wholesale Power Markets were introduced in England in 1990 and in the US in 1997 [4]. Competitive Wholesale Power Markets rely on participant bids and offers to discover dynamic LMPs that promote efficient and reliable service with fewer capacity reserves, provide location incentives that relieve transmission congestion, lower supply cost to consumers, and more.

We argue that Wholesale Power Market benefits can be enhanced significantly by short-term marginal-cost-based Distribution network Locational Marginal Prices (DLMP) enabling extensive load-side market participation. In particular, we note that distribution network costs, accounting for as much as 35% of low voltage power costs, are priced today at their average cost. The practice of average-cost-pricing deprives millions of consumers from the opportunity to match their preferences to distribution system marginal costs. As such, average-cost-pricing wastes the opportunity to capture significant cost reducing efficiencies and to realize synergies that mitigate the cost of clean but volatile and uncontrollable renewable generation.

Critical developments have taken place since wholesale power markets made their debut. Affordable communication, computation, sensing, actuation, and the advent of flexible loads and ubiquitous power electronics advocate major power market reform. The potential of smart appliance and flexible load demand response has been recognized and studied extensively under DOE funding by PNNL and collaborators [5]. We note, however, that research to date, has focused on either direct coupling of flexible loads with volatile renewable generation, or on central Utility control.

This paper is complementary in scope to this research. It focuses on the extension of LMP principles to (i) incorporate marginal costs of real and reactive power, line losses, voltage control, and distribution asset life degradation, and (ii) enable medium and low voltage consumers, distributed generation and resources to pursue their individual preferences and objectives while providing cost-effective reactive power compensation, voltage control and line loss reduction. The proposed spatiotemporal marginal cost based retail market is a process that leads diverse participants to reach consensus on the socially optimal real and reactive power prices. With this paper we aspire to contribute to the debate on whether detailed DLMP-based markets are worth considering, designing and establishing. To this end, we propose an explicit market clearing problem and solve it for a realistic distribution network feeder adopted from Southern California Edison data [6] and several scenarios of distributed market participants including conventional and flexible loads, PV generation, EV battery charging and accompanying power electronics. Scenario specific solutions yield spatiotemporally varying real and reactive power prices that are consistent with each market participant's capabilities and preferences. As such, real and reactive power DLMPs reflect market participant consensus on distributed yet coordinated individual behavioral decisions [26].

More specifically, we solve for day-ahead 24 hour DLMP price trajectories and the real and reactive power quantities consumed or produced at each point in the network, so as to minimize the distribution network operator's cost minus distributed participant benefits subject to full AC load flow relations and voltage magnitude constraints.

Related work considering distribution network costs and benefits modeled amongst others by employing AC load flow has been reported in the literature. Low and collaborators [6] focus on line loss minimization. Wang, [24], examines optimal distributed generation location. Several researchers have investigated distribution network pricing [15-23] based on locational marginal costs incorporating line losses, reactive power compensation and related costs, as well as the opportunity cost (or utility loss) of curtailing consumption. In this paper we present a comprehensive model of distribution network capabilities, distribution operator variable costs, and market participant capabilities, costs and preferences. In particular:

A. We model
- The opportunity cost of reactive power compensation at the substation,
- Transformer loss of life,
- Flexible loads, such as EVs, that co-optimize the coupled trajectories of charging their battery and the excess power electronics capacity which is put to dual use for reactive power compensation and voltage control and line loss reduction
- Non-dispatchable PV generation with power electronics/inverters whose excess capacity can be put to dual use for reactive power compensation, voltage control and line loss reduction
- Distributed Capacitors at fixed locations which can operate either in an on/off or continuous mode and produce reactive power for voltage control, and line loss reduction.

B. We Use Optimality Conditions to Unbundle DLMPs to Building Blocks associated with
- The wholesale Transmission Market LMP at the substation,
- Substation real and reactive power costs,
- The loss of distribution network asset life, and, most importantly,
- Voltage control related congestion costs.

This unbundling enables interesting analysis of the allocation of gross revenues amongst centralized generation and transmission, distribution network assets, as well as distributed resources and loads.

C. We evaluate report and analyze DLMP trajectories across several load and resource scenarios which
- Elaborate the usefulness of both real and reactive power dynamically changing DLMPs, which, if communicated widely, promote efficient, in fact optimal, operation of distribution network participants including load response, flexible load scheduling, EV battery charging, and the utilization of distributed resource and power electronics for voltage control and reactive power compensation,
- Demonstrate the sensitivity of DLMPs to network asset capabilities, the location, flexibility and controllability of loads and distributed resources. As such, DLMPs are shown to encourage optimal location, sizing, installation timing and hence technology mix of distribution network loads, distributed generation and resources.
- Support the conclusion that operational and longer term decision impacts of DLMPs on distributed loads and resources may have a profound influence on distribution infrastructure design and resilience to evolving and growing distribution service requirements.

The rest of this paper is organized as follows. Section II defines variables, formulates the market clearing problem and derives the unbundling of DLMPs. Section III describes a realistic distribution feeder consisting of industrial commercial and residential sub-feeders and employs it to quantify day ahead market DLMP trajectories at several hundred busses and the distributional aspects of DLMP unbundling. Numerical results reported, discussed and analyzed in section IV elaborate several key aspects of DLMPs and their effectiveness in promoting distribution network infrastructure resilience through distributed generation and resource integration. Section V concludes and discusses interesting ongoing and future work on the scalability and tractability of the DLMP market clearing problem. Appendices following the reference list provide the detailed input used to characterize the distribution feeder and several scenarios of PV, EV, distributed Shunt capacitors and the controllability of shunt capacitors and power electronics accompanying PV and EV that is employed in employing them for reactive power compensation and Voltage control.

II.   THE DISTRIBUTION DAY-AHEAD MARKET CLEARING PROBLEM

A. Notation Conventions

General

ε: Arbitrarily small positive quantity.

$1_{condition}$: Indicator function. When its subscript holds true, the value of the indicator function is 1, else it is 0.

h: argument indicating a specific hour in the day ahead market, h=1,2,3,…,24.

Distribution Network related Subscripts and Sets
b, b': Subscripts denoting a typical bus.
∞: Subscripts denoting the substation
(b, b'): Subscripts denoting a line connecting bus b to bus b'.
d_i, g_i, f, e_i: Subscripts denoting respectively a specific distributed load, distributed generation, shunt capacitor, and distributed power electronics. For example, $d_i(b)$ means that load d_i is located at bus b.
$\{\ell\}, \{tr\}$: Sets indicating lines and transformers in the distribution feeder topology.

Load/Generator utilities/costs capacities, Admittances
$c_{g_i(b)}, u_{d_i(b)}$: Marginal Cost, Utility, associated with generation, load type g_i, d_i located at bus b.
c_∞^V: cost of square substation-voltage-deviations from the nominal voltage level.
c_∞^G: Marginal cost of Generation at the Substation.
$\hbar(Q_\infty(h))$: fuel cost of Substation Generator associated with producing reactive power $Q_\infty(h)$. This is generally much smaller per MVAr than c_∞^G, and can be practically ignored.
$C_\infty, C_{g_i(b)}, C_{f(b)}, C_{e_i(b)}$: Capacities of substation bus generator, distributed generator g_i, capacitor f and power electronics e_i located at bus b.
$\mathbf{G}, \mathbf{B}$: Matrices whose elements $G_{b,b'}, B_{b,b'}$ denote respectively the real and imaginary components of line or transformer admittance. $G_{b,b'}, B_{b,b'}$ are defined for all (b, b') pairs, but are only non-zero when the buses b and b' are connected directly. As such zero and non-zero elements define the topology of the distribution network.

Network Load Flow variables
P, Q, S: real, reactive and apparent power, respectively. For example $P_{d_i(b)}$ denotes real power withdrawn from bus b by distributed load d_i connected at bus b.
$A_b(h), V_b(h)$: voltage angle and magnitude at bus b during hour h.
$\phi_{d_i(b)}$: fixed (+ or -) Current/Voltage phase shift introduced by (capacitive or inductive) load d_i connected to bus b.

Electric Vehicles
τ: EV departure time (EV departs at the beginning of hour $h = \tau$)
h_{arr}: Time of arrival of EV (EV arrives at the beginning of hour $h = h_{arr}$)
$i(\tau)$: Superscript denoting charging EV with departure deadline τ. The EV's loss of utility depends on its battery's state of discharge during hour h=τ.
$x_{i_{\tau, h_{arr}}(b)}(h)$: State of discharge of EV i connected to bus b with desired departure at time τ and arrival time h_{arr}.
$u_{i_{\tau, h_{arr}}(b)}(x_{i_{\tau, h_{arr}}(b)}(\tau))$: Loss of Utility (cost) to EV wishing to depart during hour τ when its discharge state is $x_{i_{\tau, h_{arr}}(b)}(\tau)$. Modeled as zero when $x_{i_{\tau, h_{arr}}(b)}(\tau) = 0$, positive otherwise.
$r_{i_{\tau, h_{arr}}(b)}$: Charging rate of EV connected to bus b wishing to depart at hour τ.

Transformers
$c_{b,b'}^{tr}$: Cost of decreasing the economic life of transformer tr by one hour. Transformers are modelled by lines $(b, b') \in \{tr\}$
$\theta_{b,b'}^H(h), \theta^A(h)$: Hottest spot, ambient temperature during hour h of transformer $(b, b') \in \{tr\}$.

$S_{b,b'}^N$: Apparent flow rating of transformer $(b,b') \in \{tr\}$.

$\Gamma_{b,b'}(\theta_{b,b'}^H(S_{b,b'}(h)))$: Loss of life of Transformer $(b,b') \in \{tr\}$, measured in hours of economic life per hour of clock time, when the apparent power flow through the transformer is $S_{b,b'}(h)$ inducing a hottest spot temperature of $\theta_{b,b'}^H(h)$.

Following [9,10], we use $\Gamma_{b,b'} = \exp(\dfrac{15000}{383} - \dfrac{15000}{273 + \theta_{b,b'}^H(h)}), \forall (b,b') \in \{tr\}$ where

$\theta_{b,b'}^H(h) = \theta^A(h) + k_{1,b,b'} + k_{2,b,b'}\left(\dfrac{S_{b,b'}(h)}{S_{b,b'}^N}\right)^2$ and $k_{1,b,b'}, k_{2,b,b'}$ are known calibration parameters while $\theta^A(h)$ is predictable for the day ahead hours.

Transmission LMPs at Transmission Network Bus where the Distribution Substation is Connected

$\pi_\infty^P(h)$: Transmission level LMP of real power during hour h at the bus where the distribution substation is connected.

$\pi_\infty^R(h)$: Transmission level clearing price of reserves during hour h at the bus that the substation is connected. Although a simple Transmission and Distribution network interface is adopted in this paper treating $\pi_\infty^P(h)$ and $\pi_\infty^R(h)$ as given exogenously, modeling the interaction of T&D decisions is possible as shown in [15].

Dual Variables

$\bar{\mu}_b(h), \underline{\mu}_b(h)$: Lagrange Multiplier of the upper and lower voltage magnitude constraints of bus b during hour h respectively. We are also using $\mu_b(h) = \bar{\mu}_b(h) - \underline{\mu}_b(h)$.

$\kappa_{f(b)}(h)$: Lagrange Multiplier of the upper limit in the utilization of a network capacitor located at bus b (see constraints 7 and 7').

B. The Market Clearing Problem

The Day-Ahead Distribution Market Clearing problem is the minimization over distribution network location-specific real and reactive power injections of:

> (*i*) the cost of real power procured at the substation, plus
> (*ii*) the cost of required voltage modulation at the substation as needed to maintain voltage levels throughout the network within acceptable bounds, minus
> (*iii*) real power consumer utility, plus
> (*iv*) the distribution operator opportunity cost associated with the production of reactive power at the substation as needed [11, 12], plus
> (*v*) substation generator reactive power production fuel costs, plus
> (*vi*) the cost of transformer loss of life, plus
> (*vii*) distributed generation costs (if any. E.g., PV generation has zero costs), plus
> (*viii*) EV uncharged battery loss of utility.

Note that the opportunity cost of reactive power compensation at the substation is either the value of lost sales to the wholesale market of real power (when $\pi_\infty^P > c_\infty^G$) or of reserves (when $\pi_\infty^P < c_\infty^G$).

The objective function described above is minimized subject to constraints (1)-(15) described in words as follows:

- AC load flow relationships, (1), (2), (8), (9) and (12)
- real and reactive power injections by loads and generators (3), (4) and (5)
- power conditioning assets accompanying loads such as asynchronous motor HVAC systems, elevator banks, PV installations, and EVs (6)
- reactive power output of shunt capacitors which depends on their location voltage (7), (7'). Whereas (7) represents on/off capacitors, (7') represents continuously controllable capacitors.
- voltage magnitude constraints (10), (11), and
- EV charge related constraints. Those are intertemporal state of charge dynamics (13), non-negativity of uncharged EV battery (14) and charging rate constraints (15). Note that similarly time coupled state dynamics can be used to represent other flexible schedulable loads such as HVAC and duty cycle appliances.

More specifically, the market clearing problem is the solution to the following constrained optimization problem:

$$\min_{P_{g_i(b)}(h),P_{d_i(b)}(h),P_{d_b^i(\tau)}(h),Q_{g_i(b)}(h),Q_{e_i(b)}(h),Q_{f(b)}(h),V_\infty(h)} \sum_h \{ \underbrace{P_\infty(h)\pi_\infty^P(h)}_{(i)} + \underbrace{c_\infty^V(V_\infty(h)-1)^2}_{(ii)} - \underbrace{\sum_{b,i\neq i^*} u_{d_i(b)}(h)P_{d_i(b)}(h)}_{(iii)}$$

$$+ \underbrace{\left[1_{\pi_\infty^P(h)>c_\infty^G}(\pi_\infty^P(h)-c_\infty^G) + 1_{\pi_\infty^P(h)<c_\infty^G}\pi_\infty^R(h)\right]\left(C_\infty - \sqrt{C_\infty^2 - Q_\infty^2(h)}\right)}_{(iv)} + \underbrace{\hbar(Q_\infty(h))}_{(v)} + \underbrace{\sum_{b,b'\in\{\text{tr}\}} c_{b,b'}^{\text{tr}}\Gamma_{b,b'}(h)}_{(vi)} \qquad (0)$$

$$+ \underbrace{\sum_{b,i} c_{g_i(b)}(h)P_{g_i(b)}(h)\}}_{(vii)} + \underbrace{\sum_{b,i_{\tau,h_{arr}}(b)} u_{i_{\tau,h_{arr}}(b)}(x_{i_{\tau,h_{arr}}(b)}(\tau))}_{(viii)}$$

Subject to

$$P_{b,b'}(h) = \left(V_b(h)\right)^2 G_{b,b'} - V_b(h)V_{b'}(h)G_{b,b'}\cos(A_b(h)-A_{b'}(h)) - V_b(h)V_{b'}(h)B_{b,b'}\sin(A_b(h)-A_{b'}(h)) \qquad (1)$$

$$Q_{b,b'}(h) = -\left(V_b(h)\right)^2 B_{b,b'} + V_b(h)V_{b'}(h)B_{b,b'}\cos(A_b(h)-A_{b'}(h)) - V_b(h)V_{b'}(h)G_{b,b'}\sin(A_b(h)-A_{b'}(h)) \qquad (2)$$

$$0 \leq \left(P_{g_i(b)}(h)\right)^2 + \left(Q_{g_i(b)}(h)\right)^2 \leq \left(C_{g_i(b)}\right)^2 \qquad (3)$$

$$\underline{P}_{d_i(b)}(h) \leq P_{d_i(b)}(h) \leq \overline{P}_{d_i(b)}(h) \qquad (4)$$

$$Q_{d_i(b)}(h) = P_{d_i(b)}(h)\tan(\varphi_{d_i(b)}) \qquad (5)$$

$$0 \leq \left(P_{e_i(b)}(h)\right)^2 + \left(Q_{e_i(b)}(h)\right)^2 \leq \left(C_{e_i(b)}\right)^2 \qquad (6)$$

$$Q_{f(b)}(h) \in [0, \min\{C_{f(b)}, C_{f(b)}V_b^2(h)\}] \qquad (7)$$

$$0 \leq Q_{f(b)}(h) \leq \min\{C_{f(b)}, C_{f(b)}V_b^2(h)\} \qquad (7')$$

$$\sum_i P_{g_i(b)}(h) + \sum_i P_{e_i(b)}(h) - \sum_i P_{d_i(b)}(h) - \sum_{i_{\tau,h_{arr}}(b)} P_{i_{\tau,h_{arr}}(b)}(h) = P_b(h) = \sum_{b'\in\{b':(b,b')\in\{\ell\}\}} P_{b,b'}(h), \forall b\neq \infty \qquad (8)$$

$$\sum_i Q_{g_i(b)}(h) + \sum_i Q_{e_i(b)}(h) + Q_{f(b)}(h) - \sum_i Q_{d_i(b)}(h) = Q_b(h) = \sum_{b'\in\{b':(b,b')\in\{\ell\}\}} Q_{b,b'}(h), \forall b\neq \infty \qquad (9)$$

$$\underline{V}_b \leq V_b(h) \qquad (10)$$

$$V_b(h) \leq \overline{V}_b \qquad (11)$$

$$A_\infty(h) = 0 \qquad (12)$$

$$x_{i_{\tau,h_{arr}}(b)}(\tau) = x_{i_{\tau,h_{arr}}(b)}(h_{arr}) - \sum_{h=h_{arr}}^{\tau-1} P_{i_{\tau,h_{arr}}(b)}(h) \qquad (13)$$

$$x_{i_{\tau,h_{arr}}(b)}(h) \geq 0 \qquad (14)$$

$$P_{i_{\tau,h_{arr}}(b)}(h) \leq r_{i_{\tau,h_{arr}}(b)} \qquad (15)$$

For the remainder of this paper we assume that the fuel cost of producing reactive power at the substation, $\hbar(Q_\infty(h))$, is small and neglect them in analytical expressions below and certainly in all numerical results reported in Section III.

C. Unbundling of DLMPs

As long as there are no multiple solutions, a condition that holds in a radial network with no loops [7, 8, 19], as is the case here, the optimal solution can be obtained uniquely and provides optimal decision variables as well as the dual variables associated with constraints (1) through (15). The real and reactive DLMP at bus b during hour h, $\pi_b^P(h)$ and $\pi_b^Q(h)$ respectively, are obtained as the Lagrange multipliers of (8) and (9).

5

At each hour h and each bus b, we consider a costless infinitesimal injection of real power $P_{\tilde{g}^P(b)}(h)$ and of reactive power $Q_{\tilde{g}^Q(b)}(h)$. As such, the market clearing problem can be rewritten as:

$$\min_{P_{\tilde{g}^P(b)}(h),Q_{\tilde{g}^Q(b)}(h),P_{g_i(b)}(h),P_{d_b^{i(\tau)}}(h),P_{d_i(b)}(h),Q_{g_i(b)}(h),Q_{e_i(b)}(h),Q_{f(b)}(h),V_\infty(h)} \quad (0)$$

Subject to (1)-(6), $(7')$, (10)-(15) and

$$P_{\tilde{g}^P(b)}(h) + \sum_i P_{g_i(b)}(h) + \sum_i P_{e_i(b)}(h) - \sum_i P_{d_i(b)}(h) - \sum_{i_{\tau,h_{arr}}(b)} P_{i_{\tau,h_{arr}}(b)}(h) = P_b(h) = \sum_{b'\in\{b':(b,b')\in\{\ell\}\}} P_{b,b'}(h), \forall b \neq \infty$$

$$Q_{\tilde{g}^Q(b)}(h) + \sum_i Q_{g_i(b)}(h) + \sum_i Q_{e_i(b)}(h) + Q_{f(b)}(h) - \sum_i Q_{d_i(b)}(h) = Q_b(h) = \sum_{b'\in\{b':(b,b')\in\{\ell\}\}} Q_{b,b'}(h), \forall b \neq \infty$$

$$P_{\tilde{g}^P(b)}(h) \leq \varepsilon \qquad\qquad (16)$$

$$Q_{\tilde{g}^Q(b)}(h) \leq \varepsilon \qquad\qquad (17)$$

By virtue of the zero generating cost, the Lagrange multiplier of (16) is the real DLMP at bus b, $\pi_b^P(h)$, and the Lagrange multiplier of (17) is the reactive DLMP at bus b, $\pi_b^Q(h)$. We append constraints to form the Lagrangian. To proceed, we note that the energy balance equations (8) and (9) are dictated by Kirchoff's laws, therefore any change in $P_{\tilde{g}^P(b)}(h)$ or $Q_{\tilde{g}^Q(b)}(h)$ on the left hand side of (8) or (9) respectively, will result in the same change in the right hand side, $\sum_{b'|(b,b')\in\{\ell\}} P_{b,b'}(h)$ or $\sum_{b'|(b,b')\in\{\ell\}} Q_{b,b'}(h)$ respectively. Therefore, (8) and (9) will not contribute any terms to $\dfrac{\partial L}{\partial P_{\tilde{g}^P}(h)}$ and $\dfrac{\partial L}{\partial Q_{\tilde{g}^Q}(h)}$. The same holds for constraints (1) and (2). Ignoring terms from (1), (2), (8) and (9), the reduced Lagrangian is as follows:

$$L = \sum_{b,i(\tau)} u_{i_{\tau,h_{arr}}(b)}(x_{i_{\tau,h_{arr}}(b)}(\tau)) + \sum_h \left\{ \begin{aligned} & \pi_\infty^P P_\infty(h) + \pi_\infty^P(C_\infty - \sqrt{C_\infty^2 - (Q_\infty(h))^2}) + \sum_{i,b} c_{g_i(b)} P_{g_i(b)}(h) + \sum_{tr} c_{tr}\Gamma_{tr}(h) \\ & + c_\infty^V(V_\infty(h)-1)^2 - \sum_{i,b} u_{d_i(b)} P_{d_i(b)}(h) \\ & + \sum_{i,b} \underline{\lambda}_{d_i(b)}(h)(\underline{P}_{d_i(b)} - P_{d_i(b)}(h)) + \sum_{i,b} \overline{\lambda}_{d_i(b)}(h)(P_{d_i(b)}(h) - \overline{P}_{d_i(b)}) \\ & + \sum_{i,b} \kappa_{e_i(b)}(h)[(P_{e_i(b)}(h))^2 + (Q_{e_i(b)}(h))^2 - (C_{e_i(b)}(h))^2] + \sum_{i,b}\kappa_{g_i(b)}(h)[(P_{g_i(b)}(h))^2 + (Q_{g_i(b)}(h))^2 - (C_{g_i(b)}(h))^2] \\ & + \sum_b \kappa_{f(b)}(h)(Q_{f(b)} - \min\{C_{f(b)}, C_{f(b)}(V_b(h))^2\}) + \sum_b \underline{\mu}_b(h)(\underline{V}_b - V_b(h)) + \sum_b \overline{\mu}_b(h)(V_b(h) - \overline{V}_b) + q_\infty(h)A_\infty(h) \\ & + \sum_{b,i(\tau)} \lambda_{d_i^\tau(b)}(h)(x_{i_{\tau,h_{arr}}(b)}(\tau) - x_{i_{\tau,h_{arr}}(b)}(h_{arr}) + \sum_{h=h_{arr}}^\tau P_{i_{\tau,h_{arr}}(b)}(h)) + \sum_{b,i(\tau)} \kappa_{d_i^\tau(b)}(h)(P_{i_{\tau,h_{arr}}(b)}(h) - r_b^{i(\tau)}) \\ & + \sum_b \pi_b^P(h)(P_{\tilde{g}^P(b)}(h) - \varepsilon) + \sum_b \pi_b^Q(h)(Q_{\tilde{g}^Q(b)}(h) - \varepsilon) \end{aligned} \right\}$$

Noting that:

- The first order optimality conditions with respect to decision variables $P_{\tilde{g}^P(b)}$ and $Q_{\tilde{g}^Q(b)}$ imply that

$$\frac{\partial L}{\partial P_{\tilde{g}^P(b)}(h)} = \frac{\partial L}{\partial Q_{\tilde{g}^Q(b)}(h)} = 0, \forall b, h.$$

- The partial derivative of all other decision variables with respect to $P_{\tilde{g}^P(b)}$ and $Q_{\tilde{g}^Q(b)}$ is zero.
- The term in the Lagrangian arising from the capacitor related constraints $(7')$, can be rewritten as:

6

$$\min\{C_{f(b')}, C_{f(b')}(V_{b'}(h))^2\} = \begin{cases} C_{f(b')}, & V_{b'}(h) \le 1 \\ C_{f(b')}(V_{b'}(h))^2, & V_{b'}(h) > 1 \end{cases} \Rightarrow$$

$$\Rightarrow \frac{\partial}{\partial P_{\tilde{g}^P(b)}(h)} \min\{C_{f(b')}, C_{f(b')}(V_{b'}(h))^2\} = \begin{cases} 0, & V_{b'}(h) \le 1 \\ 2C_{f(b')}V_{b'}(h)\dfrac{\partial V_{b'}'(h)}{\partial P_{\tilde{g}^P(b)}}, & V_{b'}(h) > 1 \end{cases}$$

- The Karush-Kuhn-Tucker optimality conditions imply that $\pi_b^P(h), \pi_b^Q(h) > 0$.

We derive that the following relationships hold for each bus b:

$$-\pi_b^P(h) = \pi_\infty^P(h)\frac{\partial P_\infty(h)}{\partial P_{\tilde{g}^P(b)}(h)} + \frac{\pi_\infty^P(h)Q_\infty}{\sqrt{C_\infty^2 - (Q_\infty(h))^2}}\frac{\partial Q_\infty(h)}{\partial P_{\tilde{g}^P(b)}(h)} + \sum_{tr} c_{tr}\frac{\partial \Gamma_{tr}(h)}{\partial P_{\tilde{g}^P(b)}(h)}$$

$$-\sum_{b'}\kappa_{f_{b'}(h)}1_{V_{b'}(h)<1}2C_{f(b')}V_{b'}(h)\frac{\partial V_{b'}(h)}{\partial P_{\tilde{g}^P(b)}(h)} + \sum_{b'}\mu_{b'}(h)\frac{\partial V_{b'}(h)}{\partial P_{\tilde{g}^P(b)}(h)}$$

Or equivalently:

$$\pi_b^P(h) = \begin{cases} \underbrace{\pi_\infty^P(h) - \pi_\infty^P(h)(\overbrace{\frac{\partial P_\infty(h)}{\partial P_{\tilde{g}^P(b)}(h)}}^{\text{marginal losses}} + 1)}_{A} \\[2em] \underbrace{-\frac{\pi_\infty^P(h)Q_\infty}{\sqrt{C_\infty^2 - (Q_\infty(h))^2}}\frac{\partial Q_\infty(h)}{\partial P_{\tilde{g}^P(b)}(h)}}_{B} \\[2em] \underbrace{-\sum_{tr} c_{tr}\frac{\partial \Gamma_{tr}(h)}{\partial P_{\tilde{g}^P(b)}(h)}}_{C} \\[2em] \underbrace{+\sum_{b'}\kappa_{f_{b'}(h)}1_{V_{b'}(h)<1}2C_{f(b')}V_{b'}(h)\frac{\partial V_{b'}(h)}{\partial P_{\tilde{g}^P(b)}(h)}}_{D1} \\[2em] \underbrace{-\sum_{b'}\mu_{b'}(h)\frac{\partial V_{b'}(h)}{\partial P_{\tilde{g}^P(b)}(h)}}_{D2} \end{cases} \qquad (18)$$

And similarly for the reactive DLMP:

$$\pi_b^Q(h) = \begin{cases} \underbrace{-\pi_\infty^P(h)\dfrac{\partial P_\infty(h)}{\partial Q_{\tilde{g}^Q(b)}(h)}}_{A} \\[2em] \underbrace{-\dfrac{\pi_\infty^P(h)Q_\infty}{\sqrt{C_\infty^2 - \left(Q_\infty(h)\right)^2}}\dfrac{\partial Q_\infty(h)}{\partial Q_{\tilde{g}^Q(b)}(h)}}_{B} \\[2em] \underbrace{-\sum_{tr}c_{tr}\dfrac{\partial \Gamma_{tr}(h)}{\partial Q_{\tilde{g}^Q(b)}(h)}}_{C} \\[2em] \underbrace{+\sum_{b'}\kappa_{f_{b'}(h)}1_{V_{b'}(h)<1}2C_{f(b')}V_{b'}(h)\dfrac{\partial V_{b'}(h)}{\partial Q_{\tilde{g}^Q(b)}(h)}}_{D1} \\[2em] \underbrace{-\sum_{b'}\mu_{b'}(h)\dfrac{\partial V_{b'}(h)}{\partial Q_{\tilde{g}^Q(b)}(h)}}_{D2} \end{cases} \qquad (19)$$

(18) and (19) imply that DLMPs can be expressed in terms of interesting cost components involving the LMP at the substation bus, the marginal cost of transformer loss of life and other distribution network constraint dual variables. More specifically, the DLMPs can be unbundled and expressed as the sum of the following components:

$$\pi_b^P(h) = A + B + C + D, \quad \pi_b^Q(h) = A' + B' + C' + D'$$

Where:

A, A' are the cost of the sensitivity of Real Power (term (i) of the objective function) at the substation (i.e., evaluated at the LMP) with respect to a costless infinitesimal injection of real, reactive power respectively at b.

B, B' are the equivalent for Reactive Power (term (iv) of the objective function).

C, C' are the cost of the sensitivity of Transformer loss of life with respect to a costless infinitesimal injection of real, reactive power respectively at b (term (vi) of the objective function).

D, D' are:

1. the cost of the sensitivity of the voltage level at b times the Lagrange multiplier of (11) minus (10), where as usual the sensitivities are with respect to a costless infinitesimal injection of real, reactive power respectively, plus
2. the cost of affecting the sensitivity of the maximum reactive power output of capacitors, if their voltage is below 1p.u. (constraints $7, 7'$)

In cases where demand is not fully met despite its high utility, or the SoD of EVs is not zero at the departure deadline hour, real and reactive power DLMPs are much higher, because the Lagrange multipliers of (10) are also very high, reflecting a loss of utility in objective function terms (iii) and ($viii$).

III. NUMERICAL IMPLEMENTATIONS

A. Input data description

In order to check the applicability of our DLMP model, we applied it to a realistic 253 bus distribution feeder. The single line approximation of the 253 bus test network is depicted in Figure 30. Our feeder includes industrial, commercial and residential sub-feeders.

For the industrial feeder (busses 2-48), the location of the inflexible loads, the photovoltaics and the capacitors is exactly the same as the Southern California Edison data published in [6].

The commercial/residential feeder is an expansion of the industrial feeder. Given the average household consumption of 10kVA and the fact that residential lines cover up to 10 houses, corresponding industrial loads were substituted by a medium to low voltage transformer and a sub-feeder line segment serving several residential loads located at additional low voltage busses. A high to medium voltage transformer was added to connect the feeders to a high voltage substation. Further information on the input data of transformers can be found in Table VII of the attached Appendix.

The capacitors and photovoltaics of the commercial/residential feeder are appropriately located as explained below in Section III.B.. Input data on the location and the size of capacitors and photovoltaics can be found in Table VI.

Figure 30 shows the expanded feeder including transformer lines, PV and capacitor locations. Low voltage sub-feeder line are as a range of bus numbers due to lack of space. All medium voltage lines are identical and have a resistance of $R = 0.2\Omega$ and a reactance of $X = 0.3\Omega$, while all low voltage lines have a resistance of $R = 0.002\Omega$ and a reactance of $X = 0.003\Omega$.

Figure 30 also highlights the busses whose DLMP values are repeated as representative results. Bus 17 is a bus in the industrial feeder, close to the substation. Bus 72 is equally close to the substation but belongs to the commercial subfeeder. Bus 43 is a bus in the industrial feeder, far from the substation. Bus 233 is a bus in the residential sub-feeder, far from the substation.

The inflexible loads in the industrial feeder are assigned flat consumption during the hours of 9am-5pm. Commercial consumption peaks during 12pm to 3pm, while residential loads peak around 6pm. All of the inflexible loads have a power factor of 0.88. We will report on the real and reactive DLMPs $\pi_b^P(h), \pi_b^Q(h)$ and also the effective price caused by the coupling of real and reactive power demand of inflexible loads through the power factor, $\pi_b^P(h) + \tan(\varphi_{d_i(b)})\pi_b^Q(h)$.

On top of the inflexible loads discussed above, in our 253 bus network, we also include time-shiftable loads in the form of Electric Vehicles. Electric vehicles connect to industrial feeder locations in two classes: the first arrives at 9 am and departs at 5 pm and the second one arrives at 5pm and departs at 1am. Electric vehicles connected to commercial locations arrive at 9am and depart at 5pm. Electric vehicles connecting to residential locations arrive at 6pm and depart at 8am. The characteristics of the electric vehicles can be found in Table VIII.

We also assume that the power electronics in the charger and AC-DC-AC converters of EVs and PVs are able to use their excess capacity for reactive power compensation and voltage control. We call that dual use. Indeed, when the sun is not high in the sky or a plugged in EV is not using all of its charger capacity, then excess power electronic capacity can be used to compensate reactive power, a service that can and should be compensated at the running reactive DLMP. We refer to PVs and EVs collectively as distributed resources.

Network capacitors are considered as a form of investment in the network from the Distribution Network Operator. Therefore, network capacitors are not remunerated for reactive power provision.

The system peak hour is the hour of the 24-hour horizon that the sum of all the loads is maximum. This occurs at 2pm, coinciding with the peak of the industrial and commercial loads, but not with the peak of the residential loads.

The substation real LMPs of each hour are typical summer day values, from ISO NE data. The hourly evolution of the demand of inflexible loads and the output of the PVs as a percentage of their capacity is shown in Table V. The PVs peak during the afternoon hours of 11am-3pm.

B. Numerical Results

Our numerical results were obtained using the AIMMS modeling framework, which provides unfailingly the unique primal and dual optimal solutions, guaranteed by the radial topology [8]. In order to investigate the potential resilience of the grid to load increases given additional distributed resources and flexible EV loads, we use network element values (line resistance and reactance, transformer nameplate rating) that were sufficient to meet low load that was in place several years in the past. We assume that, at that time, there were no network capacitors, no PV and no time-shiftable EVs possessing power electronics that can be put to dual use for reactive power compensation. After a load increase of 40%, the network is not functional as is, and we investigate the following steps to increase its functionality:

- Providing either real power only or reactive power only from distribution level resources, i.e. resources located in busses other than the substation:
  - o We first allow the use of PV only. PV in the industrial feeder is located as in [6]. We place PV in the commercial/residential feeder close to the busses where most load is shed. We gradually increase their capacity and monitor its benefits.
  - o We then disallow the use of PV and allow the use of Network capacitors only. Capacitors in the industrial feeder are placed exactly as in [6]. In the commercial/residential feeder, they are again selectively placed close to busses where more load is shed. We gradually increase the network capacitor size and monitor the benefits.
- We investigate the case of simultaneous real and reactive power provision from distribution level resources. Real power can be provided through PVs and reactive power can be provided either through network capacitors or through putting the power electronics in PV and EVs to dual use. We gradually increase the PV levels and/or the network capacitor size and allow or disallow the dual use of the power electronics in PV and EVs.
- As mentioned above, network capacitors are an investment to the distribution system by the Distribution Network Operator. We investigate the case of using dual use of power electronics in PVs and EVs as the only means of reactive power provision other than the substation. This will compare the benefits of organically offering reactive power compensation throughout the network.

We initially solve the 24 hour Day-Ahead Market clearing problem on the test Distribution Network without any distributed resources and with peak real demand values corresponding to Table III. Table I below shows indicative results for this case.

Total Cost ($)	37016
Average Real Energy Price ($/kWh)	0.0957
Maximum Real DLMP at system peak hour ($/kWh)	0.1395
Maximum Reactive DLMP at system peak hour ($/kVarh)	0.0567

TABLE I. Indicative results for the case of fixed loads.

With a projected annual increase of 3.5%, within 15 years, the peak load values of Table III will rise to the peak load values of Table IV. In this case, without additional investment in the network, the market clearing problem will be infeasible for fixed loads, meaning that the increased load cannot be met. Table II below shows indicative results for the case of increased demand.

Total Cost ($)	65576.76
Percent of Load Shed at system peak hour (%)	6.573%
Average Real Energy Price ($/kWh)	0.3350
Maximum Real DLMP at system peak hour ($/kWh)	1.1564
Maximum Reactive DLMP at system peak hour ($/kVarh)	2.1125

TABLE II. Indicative results for increased demand.

We notice that the requisite load shedding leads to extremely high real and reactive DLMPs. In order to ameliorate load shedding, we place photovoltaics, by noting the busses where more load is shed, i.e. where the real and reactive DLMPs are highest. Figures 1 and 2 below show the real and reactive DLMPs, while figure 3 shows the effective price for increasing photovoltaic capacity.
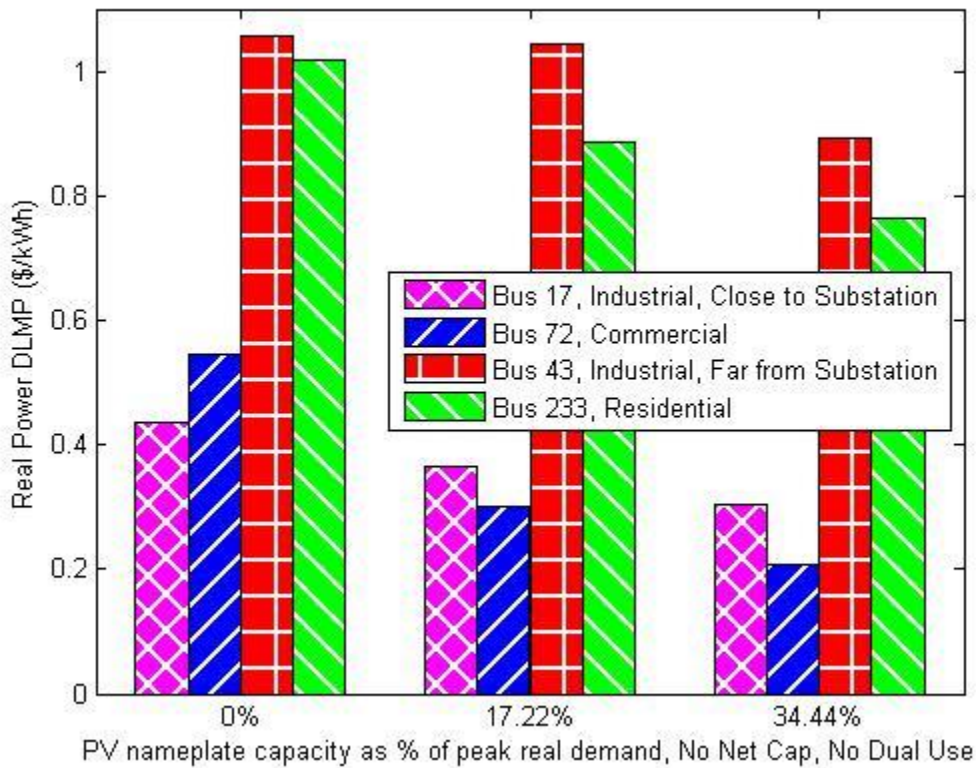
Figure 1. System Peak Hour Real DLMPs versus increasing photovoltaics capacity, No Network Capacitors, No Dual Use.
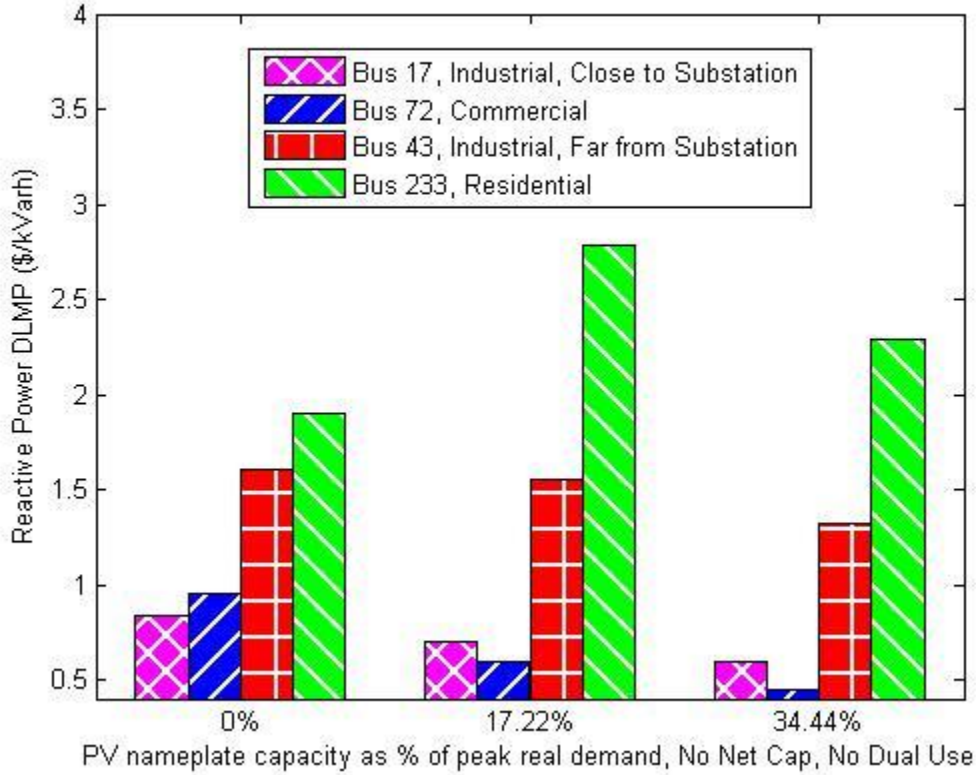
Figure 2. System Peak Hour Reactive DLMPs versus for increasing photovoltaics capacity, No Network Capacitors, No Dual Use.
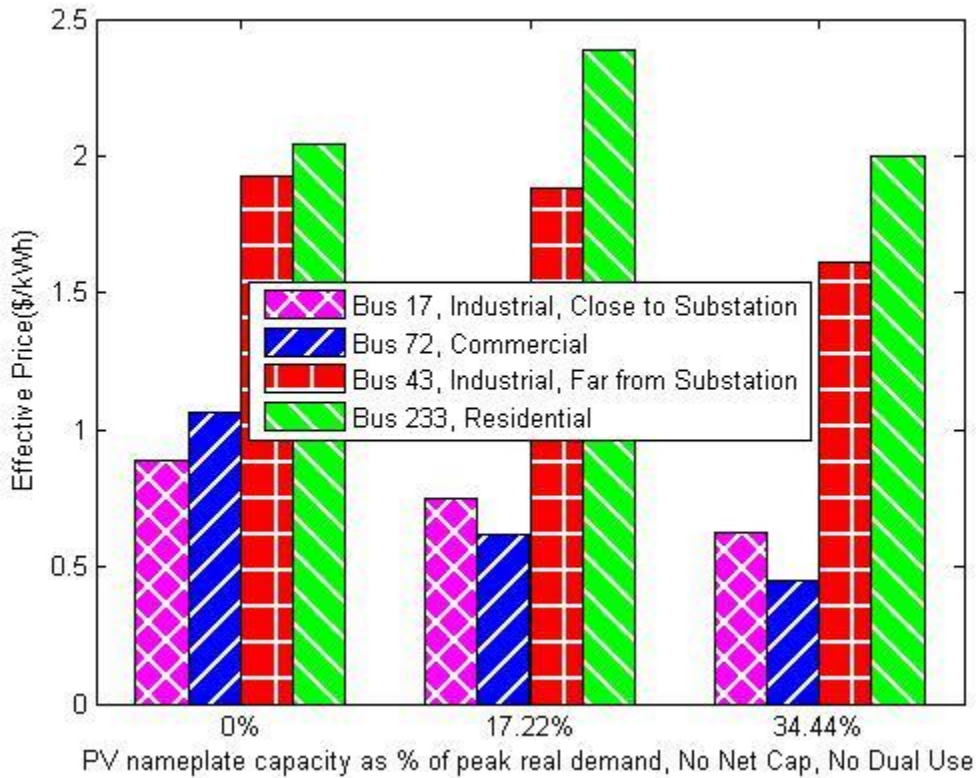
Figure 2. System Peak Hour Effective price versus for increasing photovoltaics capacity, No Network Capacitors, No Dual Use.

We notice that DLMPs are high and demand is curtailed even when PV penetration levels are as high as 34.44% of the maximum total real demand during the system peak hour. The reason for demand curtailment in these cases turns out to be the binding voltage magnitude constraints shown in Figure 4. Voltages are restricted within ±10%, and the voltage at many busses is binding, even though the voltage at the substation bus (Bus 1) is at the upper bound. Reactive DLMPs are higher than the real DLMPs, since (see terms D_1, D_1') the non-negative dual variable of the binding voltage constraints is multiplied by $\dfrac{\partial V_{b'}}{\partial Q_{\tilde{g}^Q(b)}} >> \dfrac{\partial V_{b'}}{\partial P_{\tilde{g}^P(b)}}$, due to the higher sensitivity of voltage level on reactive power. Therefore, excessive PV real power generation is discouraged by diminishing returns.
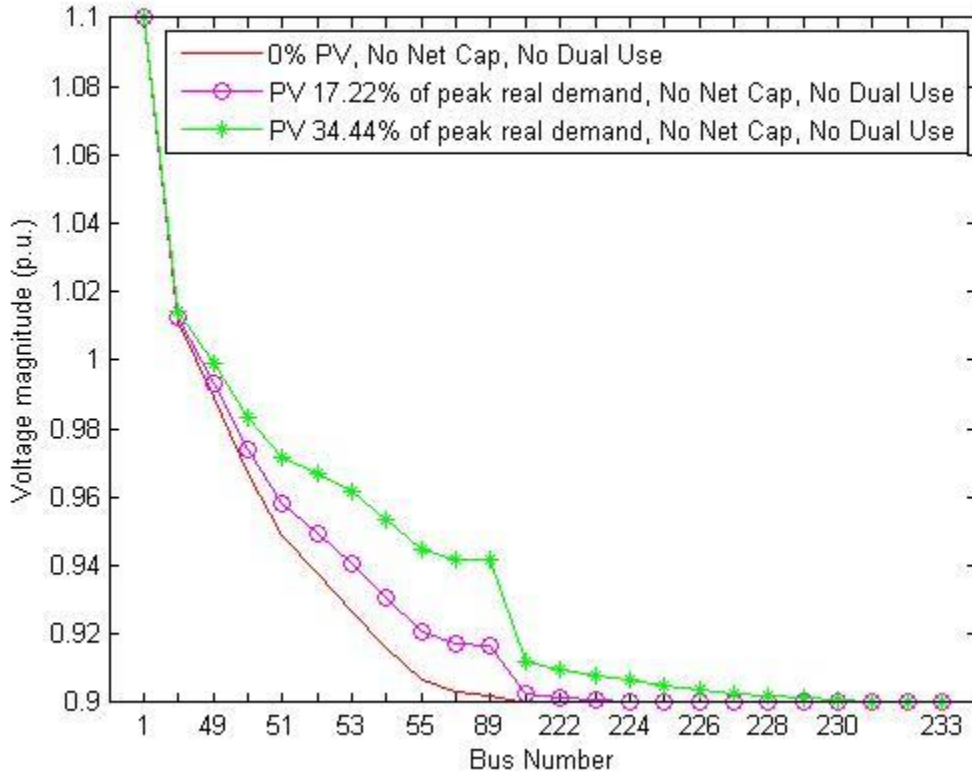
Figure 4. Voltage magnitudes decline to the lowest allowable level at busses further and further away from the substation despite higher PV capacity.

We move on to investigating the case of increasing network capacitor size, without having any distributed resources. In order to ameliorate load shedding, we place network capacitors, by noting the busses where more load is shed, i.e. where the real and reactive DLMPs are highest. Figures 5 and 6 below show the real and reactive DLMPs and Figure 7 shows the effective price for increasing network capacitor size. The combined effect of capacitors on voltage control and reactive power compensation reverses demand rationing and real and reactive DLMPs take moderate values. This demonstrates the significance of reactive power provision at distribution networks and, as such, the importance of equivalent services obtainable from dual use of accompanying power electronics. As expected, reactive power DLMPs are more sensitive on the use and size of network capacitors than real DLMPs are.
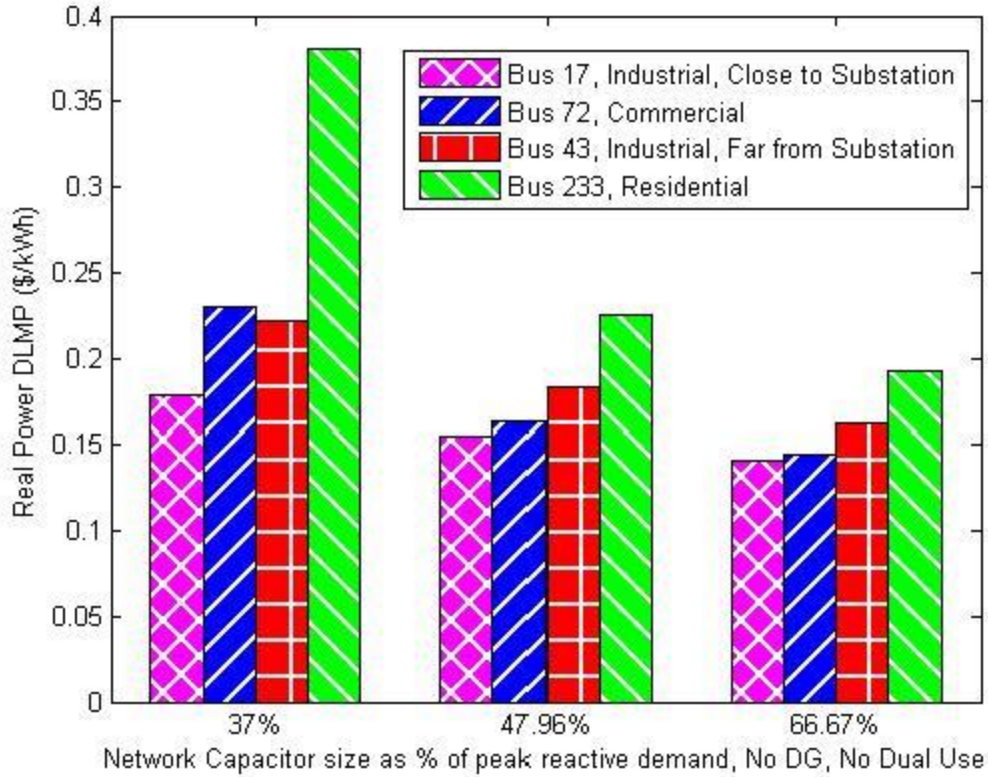
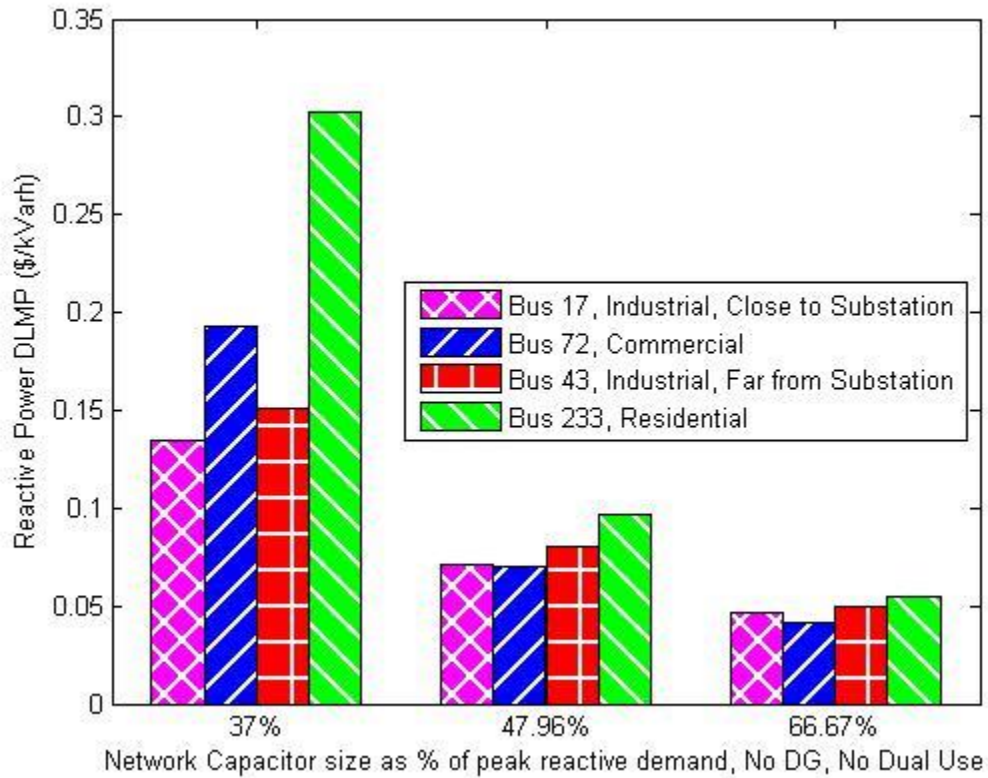Figure 5. System Peak Hour Real DLMPs versus increasing network capacitor size, No DG, No Dual Use.

Figure 6. System Peak Hour Reactive DLMPs versus increasing network capacitor size, No DG, No Dual Use.
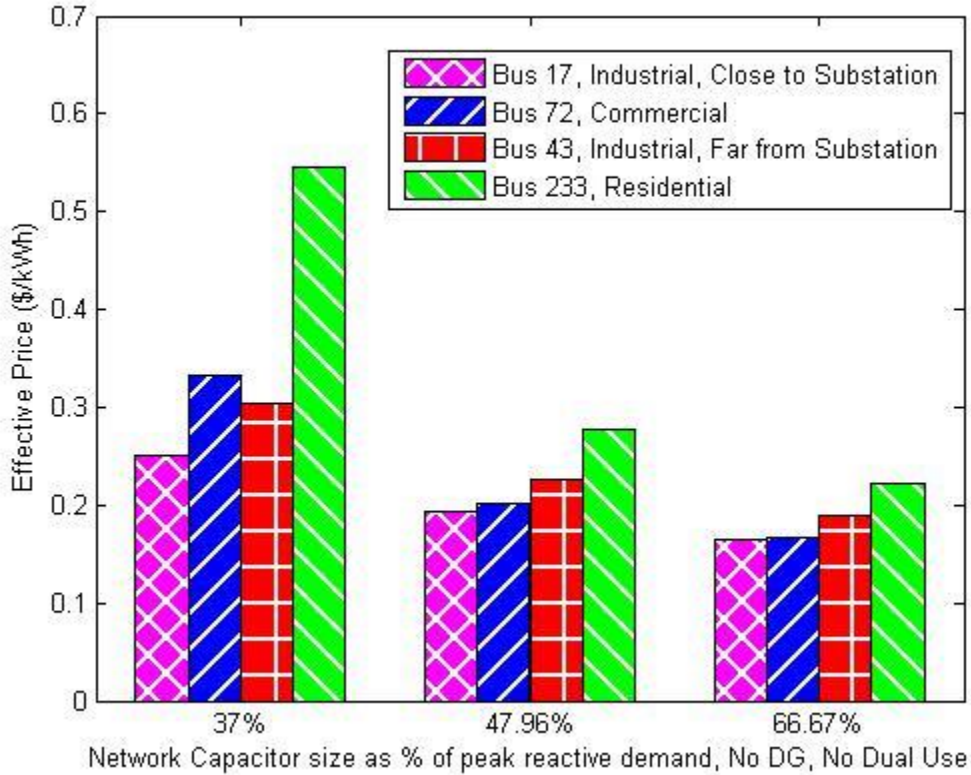
Figure 7. System Peak Hour effective price versus increasing network capacitor size, No DG, No Dual Use.

We model next scenarios where real power produced by PV and consumed by EV battery charging is associated with reactive power compensation by the dual use of accompanying power electronics. We present numerical results that quantify the sensitivity of DLMPs to different levels of which network capacitors and PVs are present in the Distribution Network as well as putting the power electronics of PV and EVs to dual use. Figures 8-10 show the real and reactive DLMPs and effective prices during the system peak hour for different PV and network capacitor levels, with or without dual use (DU) of power electronics.
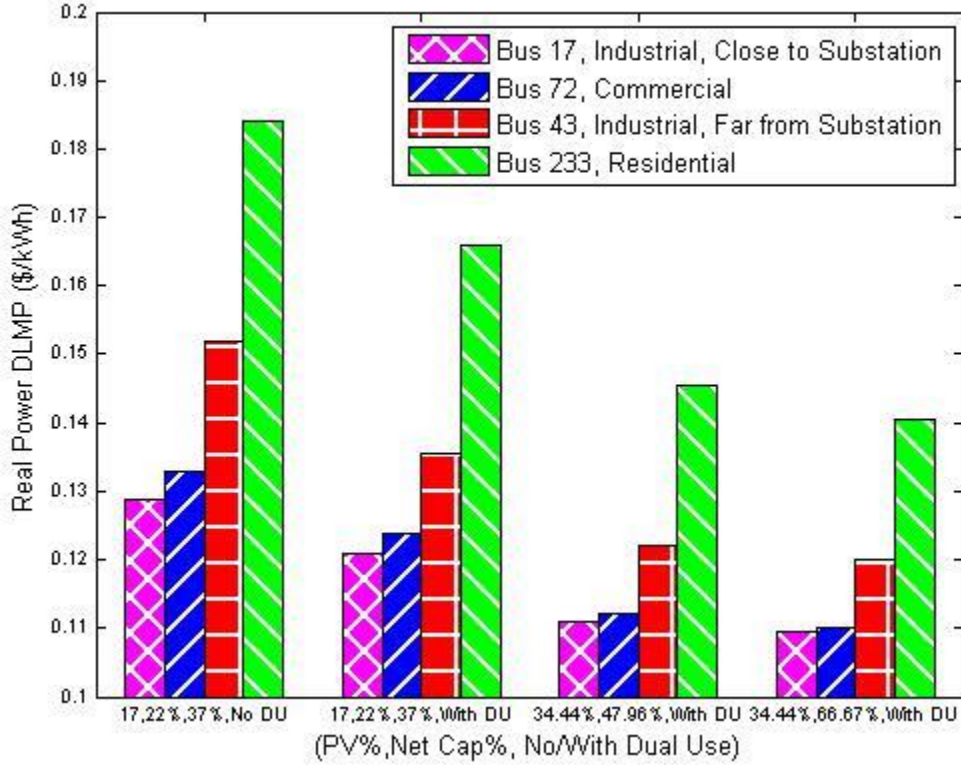
Figure 8. System Peak Hour Real Power DLMPs versus PV capacity and Network Capacitor size, with or without Dual Use.
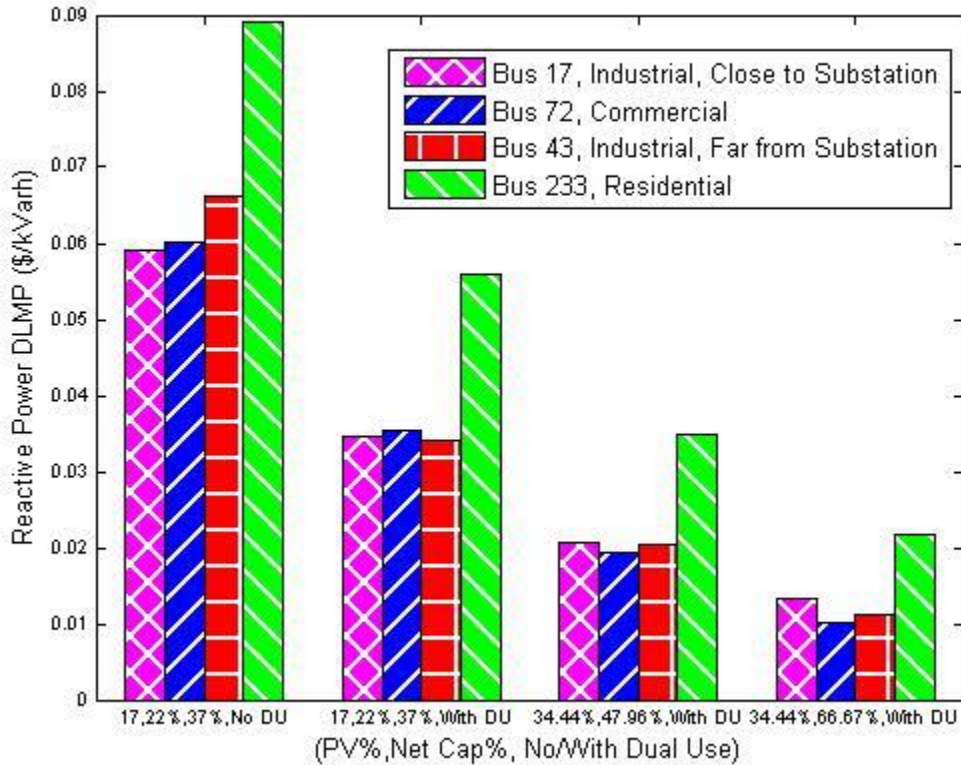
Figure 9. System Peak Hour Reactive Power DLMPs versus PV capacity and Network Capacitor size, with or without Dual Use.
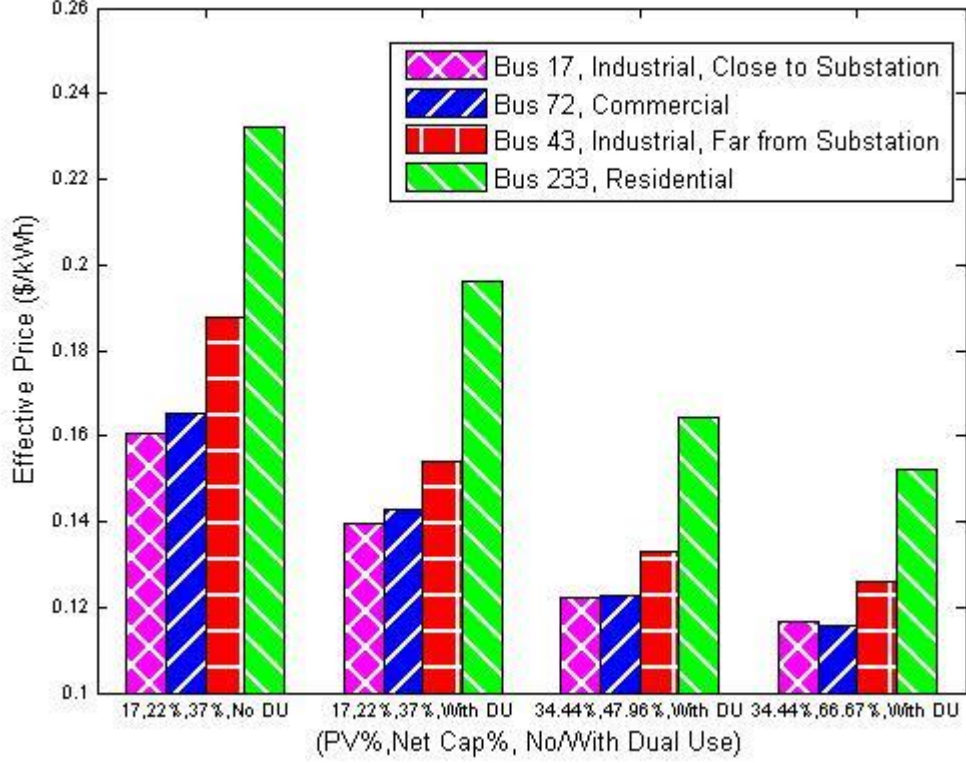
Figure 10. System Peak Hour Effective Price versus PV capacity and Network Capacitor size, with or without Dual Use.

Based on Figures 1- 3 and 5-10 above, we conclude that the real and reactive DLMPs of busses at the residential feeder are always going to be higher than those of busses in the industrial feeder and equally far from the substation and also from commercial busses in the same feeder. This is because of the involvement of the medium to low voltage transformers. However, in the industrial feeder, the relationship between the real and reactive DLMPs of busses with different distances from the substation might not always be intuitive, because of the real and reactive injections of the distributed energy resources.

In our test distribution network, inflexible loads are assigned a constant power factor of 0.88 and as such consume both real and reactive power. Therefore, they are responsible for causing higher line losses, increasing transformer degradation and voltage dips that raise the need for action to achieve voltage control. It is therefore reasonable to charge them the associated marginal costs. Therefore, demand pays the DLMP at its connection bus, in accordance to the wholesale transmission markets where load pays the LMP. Figures 11 and 12 show the total daily demand side payments,

$$x_1 = \sum_h \sum_b \left\{ \pi_b^P(h) \sum_i P_{d_i(b)}(h) + \pi_b^Q(h) \sum_i Q_{d_i(b)}(h) \right\}$$, and the average demand side payments,

$$x_2 = \frac{\sum_b \left\{ \pi_b^P(h) \sum_i P_{d_i(b)}(h) + \pi_b^Q(h) \sum_i Q_{d_i(b)}(h) \right\}}{\sum_{b,i} P_{d_i(b)}(h)}$$, respectively.
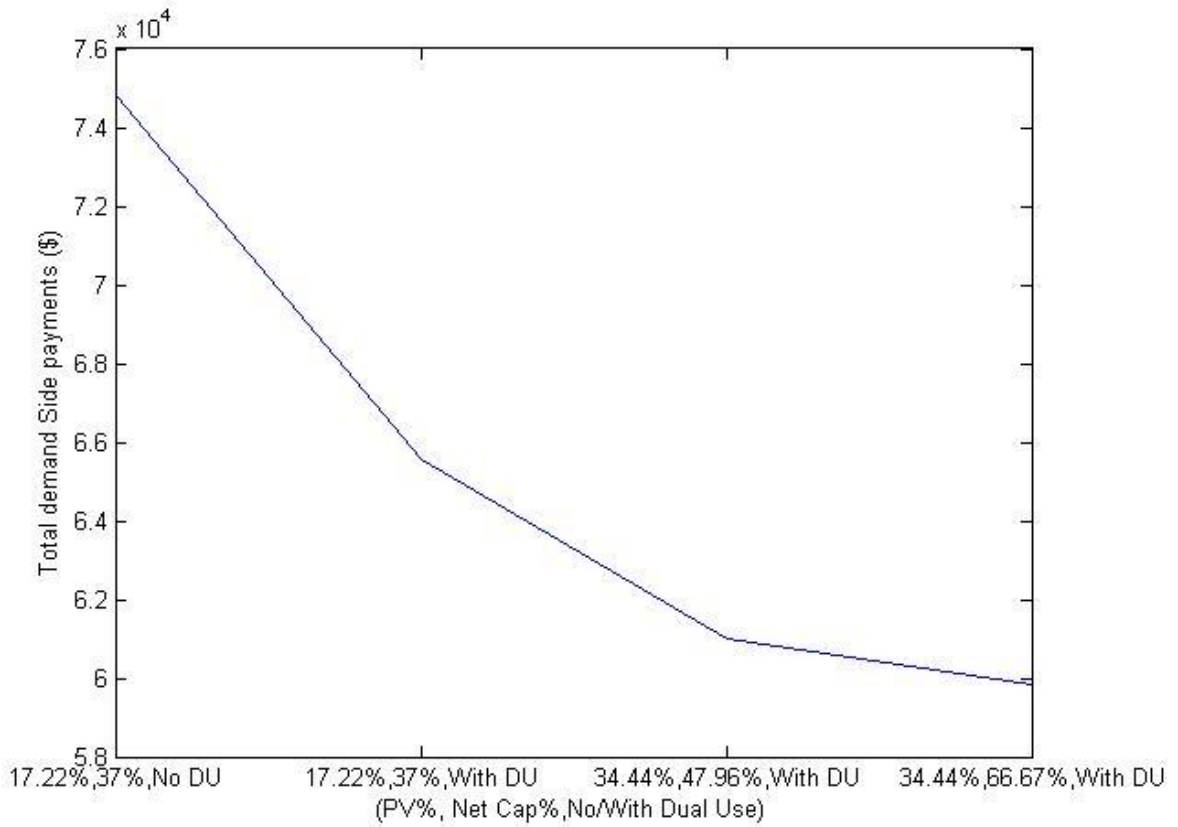
16

Figure 11. Demand Side Payments for different PV and capacitor levels.
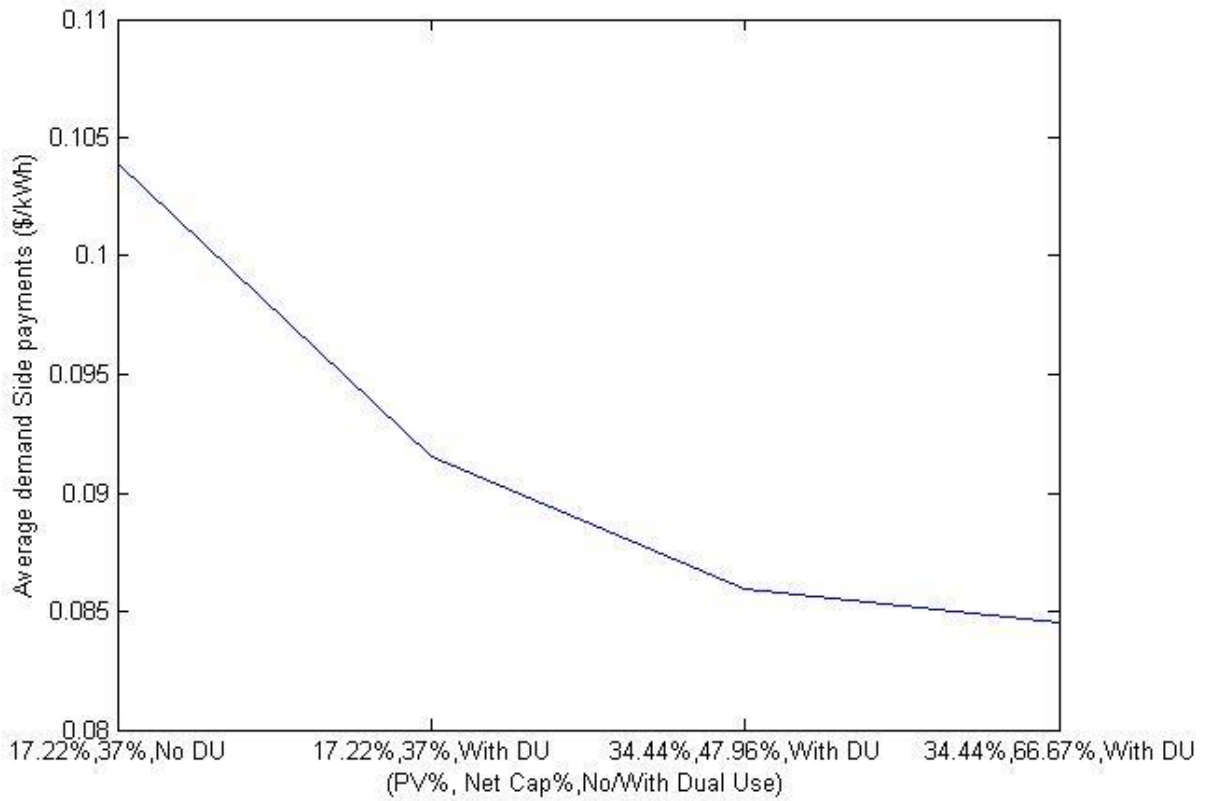

Figure 12. Average Demand Side Payments for different PV and capacitor levels.

17

On the other hand, the power electronics in EV chargers and PVs have combined inductor and capacitor capabilities. If equipped with the appropriate controller, they can be guided by the reactive power DLPM to produce rather than consume reactive power and compensate for the cost imposed by consumers of reactive power. It is therefore not only reasonable but also socially optimal to compensate power electronics with the marginal avoided cost rate quantified by the real and reactive DLMP at their location. Therefore, generation gets remunerated at the DLMP in accordance to the wholesale transmission markets where generation gets remunerated at the LMP. The income of these resources is shown in Figure 13 below.
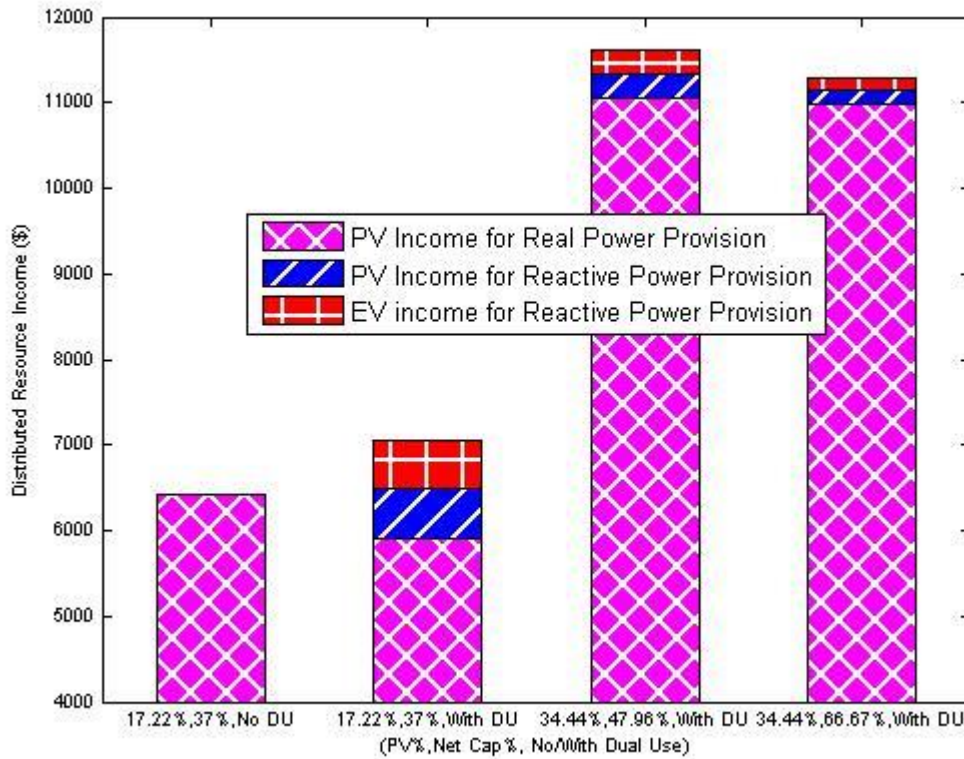

Figure 13. Distributed Resource Income for different PV and capacitor levels.

The PV and EV income results quantify the value of putting power electronics to dual use. This income can be interpreted as a market signal to make investment decisions in resource type/provision, size and location [6, 24].

The Distribution Network Operator collects the demand side payments (Figure 11), and has to cover the substation related costs (terms (*i*), (*ii*) and (*iv*) of the objective function), the equipment degradation costs (term (*vi*) of the objective function) and remunerate the power electronics for their participation in real and reactive power provision (Figure 13). Figures 14 and 15 show the substation and degradation related costs, by means of sum and percentage of the total respectively. Figure 16 shows the net income (receipts minus payments) of the DNO, as a percentage of the total costs the DNO incurs.
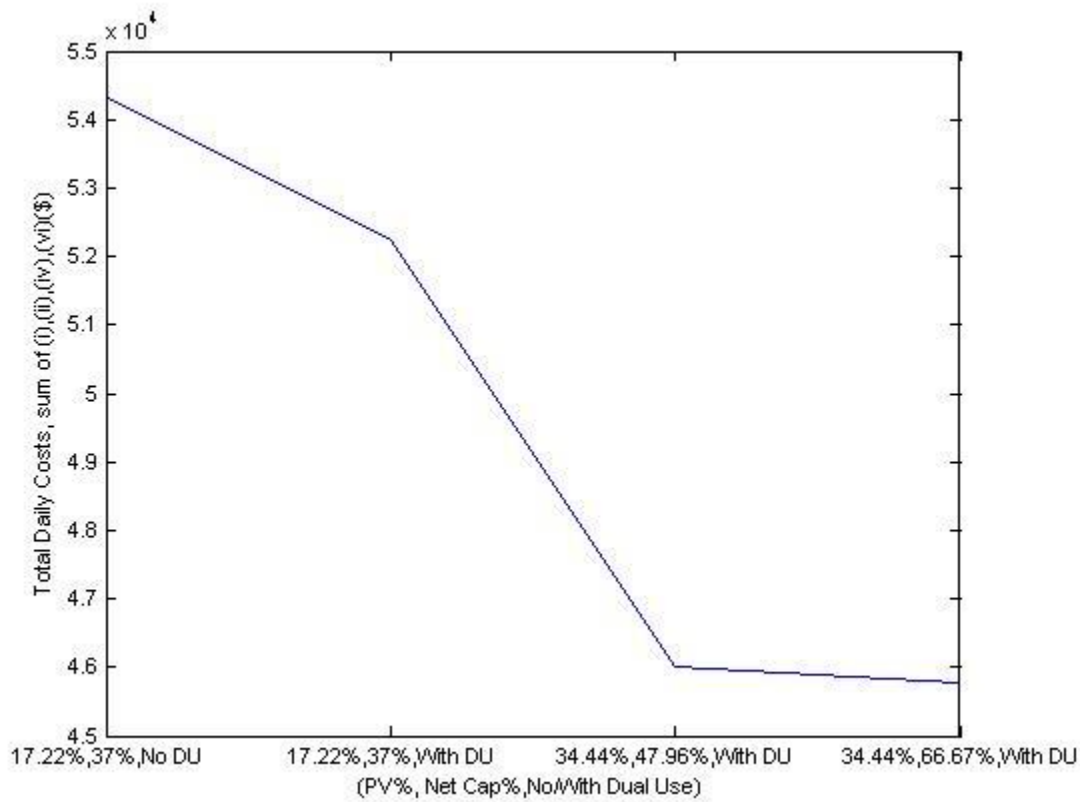
Figure 14. Total daily costs as a sum of objective function cost terms (i), (ii), (iv) and (vi) for different PV and capacitor levels.
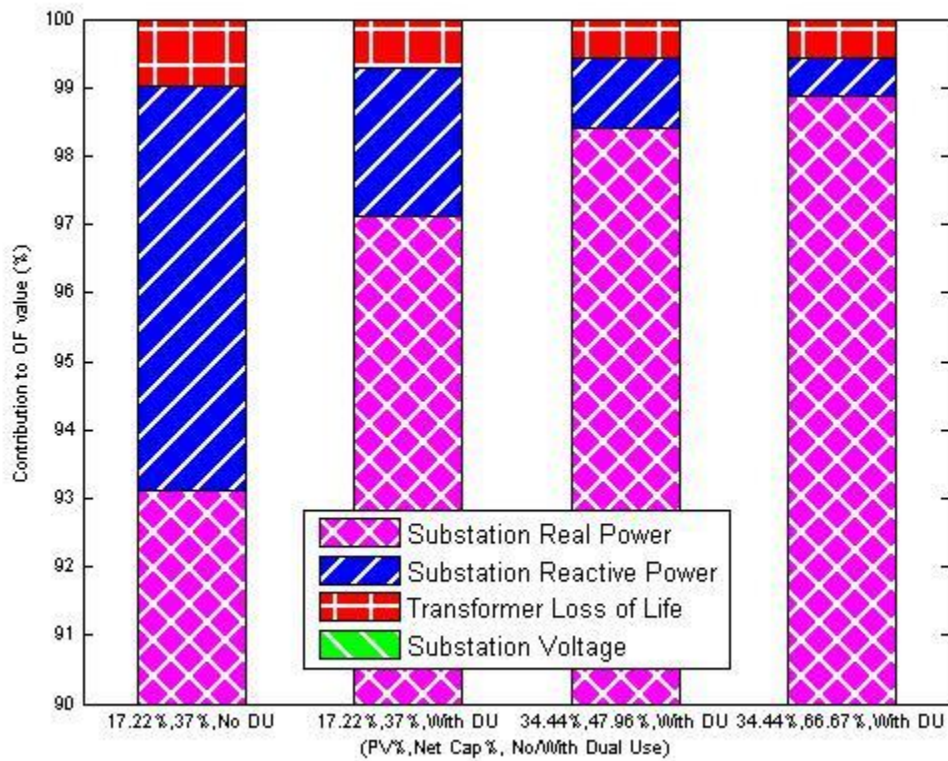

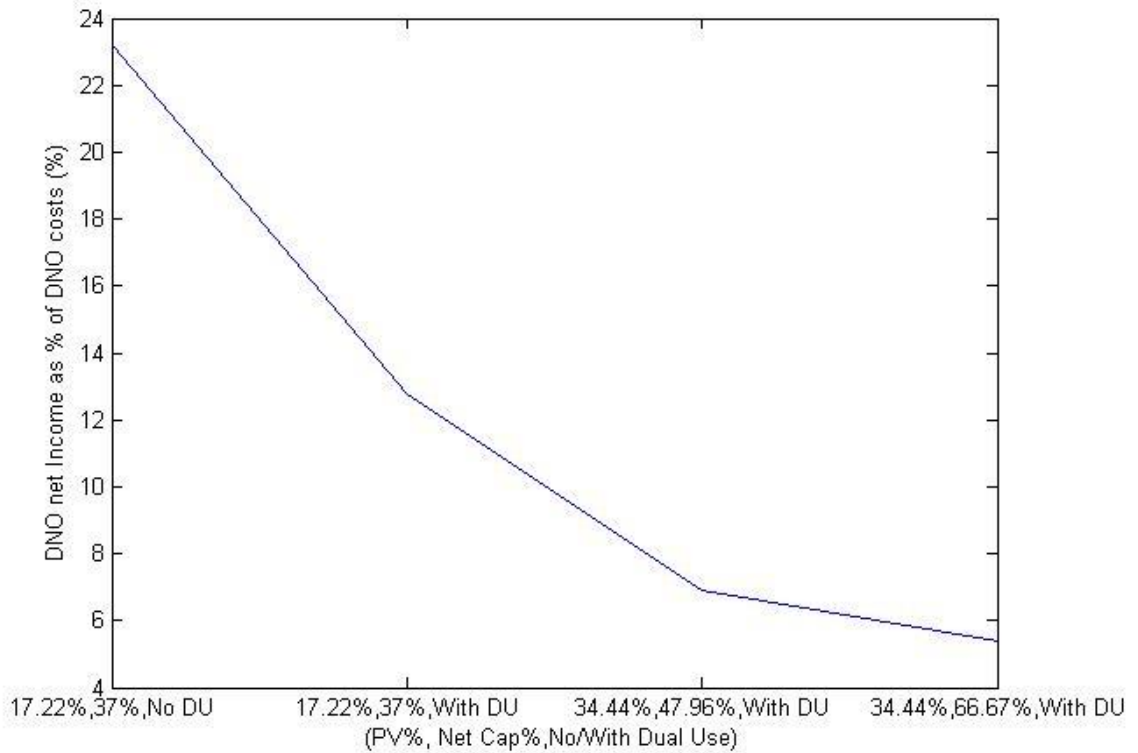Figure 15. Contribution of each objective function term for different PV and capacitor levels.

Figure 16. Distribution Network Operator Net Income as a percentage of their incurred costs for different PV and capacitor levels.

From Figure 15, we notice that several cost components not explicitly priced in today's markets, like reactive power and equipment loss of life, can be significant components of the total costs. Also, as we allow more distributed recourses, the value of the objective function decreases, but the individual cost components can increase. For example, transformer loss of life costs might increase because of the real and reactive injections of the distributed resources that have to flow through the transformers.

Figure 17 below shows the 24 hour trajectory of the maximum reactive DLMP in the network for all different PV and network capacitors levels.
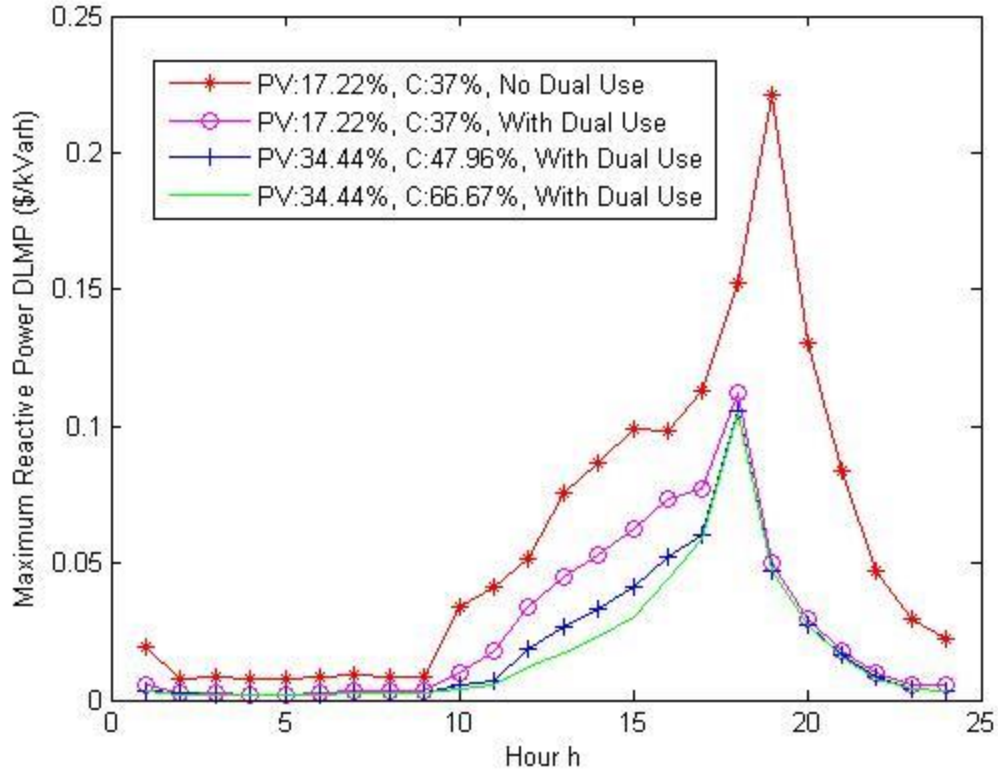
Figure 17. Maximum Reactive DLMPs of all hours for different PV and capacitor levels.

As mentioned before, the introduction of reactive power providing distributed resources results in significantly lower reactive DLMPs. When reactive power providing resources are allowed, the highest reactive DMLP during off-peak hours can be less than $1 \frac{cent}{kVarh}$. Figure 18 below shows that the usefulness of reactive power capacity (dual use and network capacitors) can saturate leading to low utilization levels, imposed amongst others by upper allowable voltage limits. Figure 19 shows that as the PV and network capacitor penetration increases, it is optimal to lower substation voltage below the maximum such that the network capacitors and power electronics can inject reactive power without driving voltages above the maximum limit. This shows the equivalence of upper voltage magnitude constraints in the distribution network and congestion constraints in the transmission level markets.
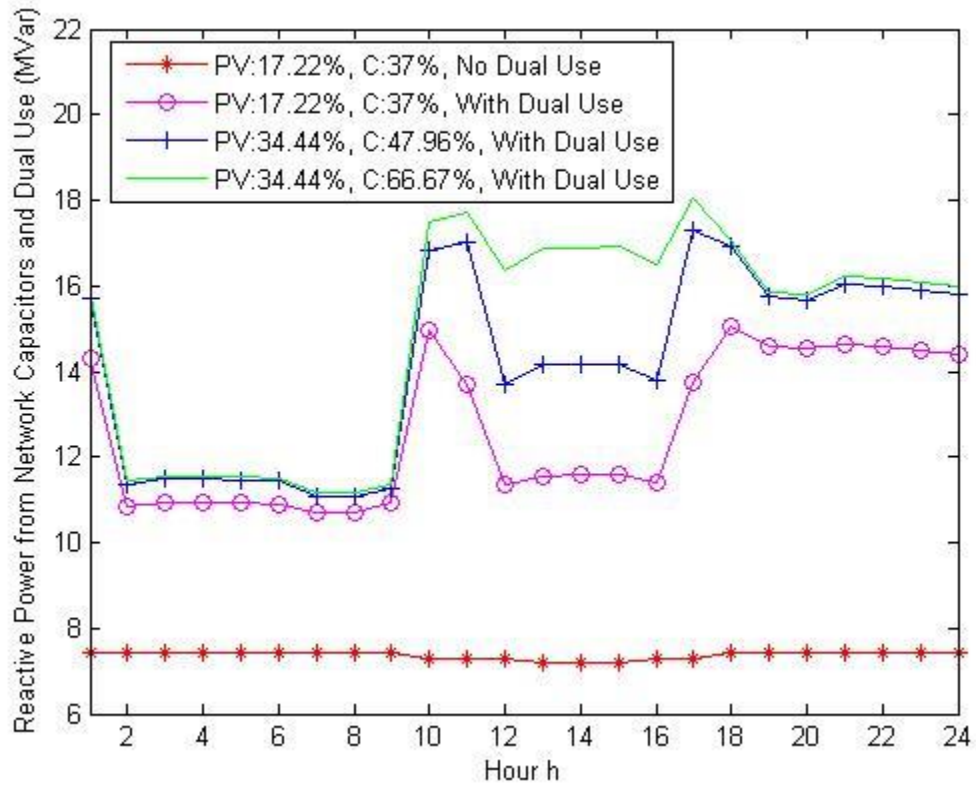
Figure 18. Reactive power provided by distributed resources per hour for different PV and capacitor levels.
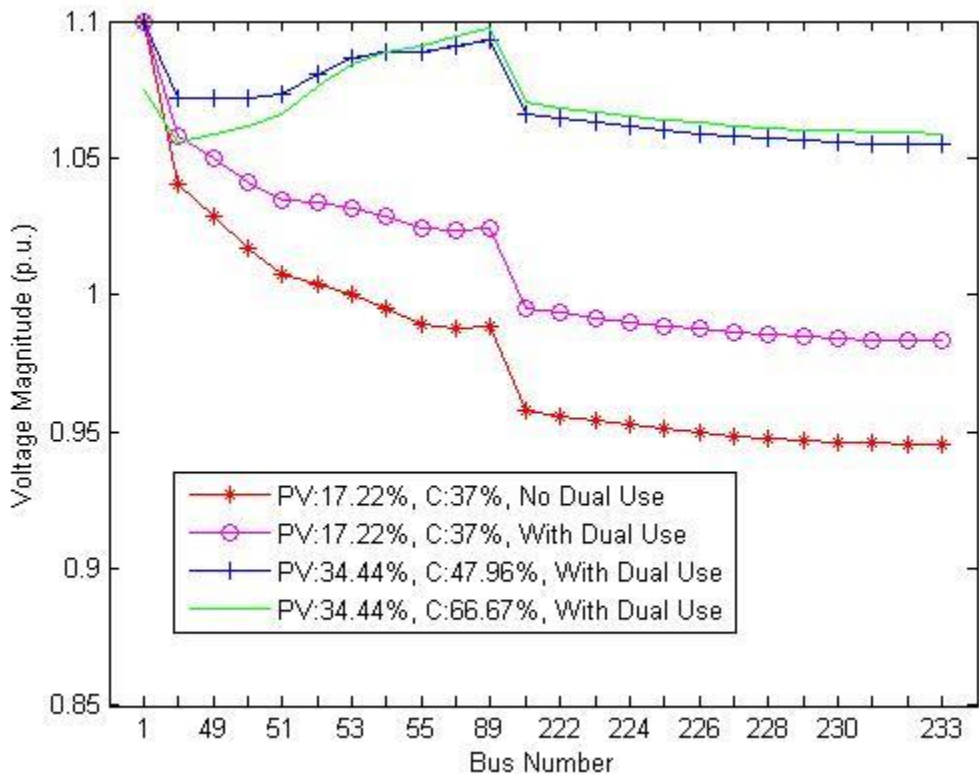

Figure 19. Bus voltage magnitudes along the line connecting bus 233 to the substation for different PV and capacitor levels.

We notice that enabling the dual use of PV and EV power electronics, allows for a flatter voltage magnitude profile, i.e. less voltage drops, throughout the line. The combined effect of voltage control and VAr compensation also means that the voltage magnitudes will be higher and line losses lower.

At any rate, however, the above results advocate that significant presence of power electronics capable of dual use renders investment in network shunt capacitors unnecessary. This leads us to investigate the resilience of the system in the case of no investment in the network from the Distribution System Operator in the form of network capacitors, i.e. when we do not have any network capacitors, but rather, we rely on the natural evolution of the system, with the penetration of photovoltaics and electric vehicles, and the dual use of their associated power electronics. We are using PV capacity equal to 25.8% of the total real power demand. This translates to about the same capacity potentially available for reactive power compensation as the case of network capacitors being 47.96% of the total reactive demand. To further support this case, we simulate a cloudy day when the photovoltaics will be unable to provide real power, i.e. there is no distributed means of real power provision, but reactive power can be provided from the power electronics of vehicles and photovoltaics. In this sense, this is much similar to having network capacitors only, as in Figures 5-7. Figures 20-23 show comparative results in demand side payments, real and reactive DLMPs and effective prices.
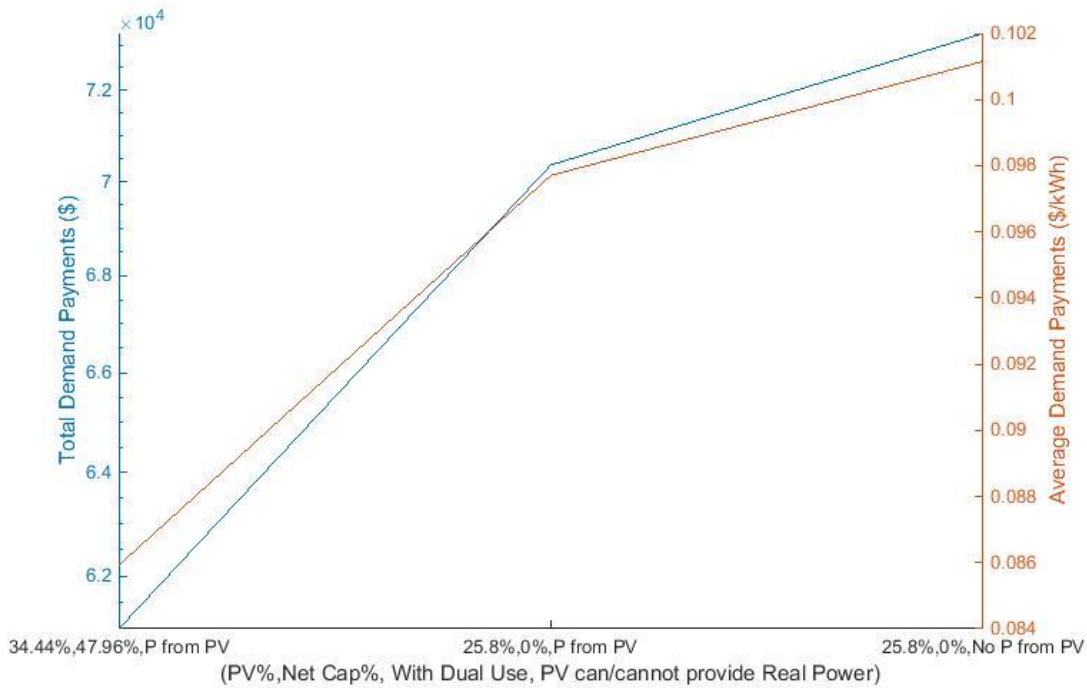

Figure 20. Total and average demand side payments in the case of No Network Capacitors, with Dual Use of power electronics in PV and EVs.
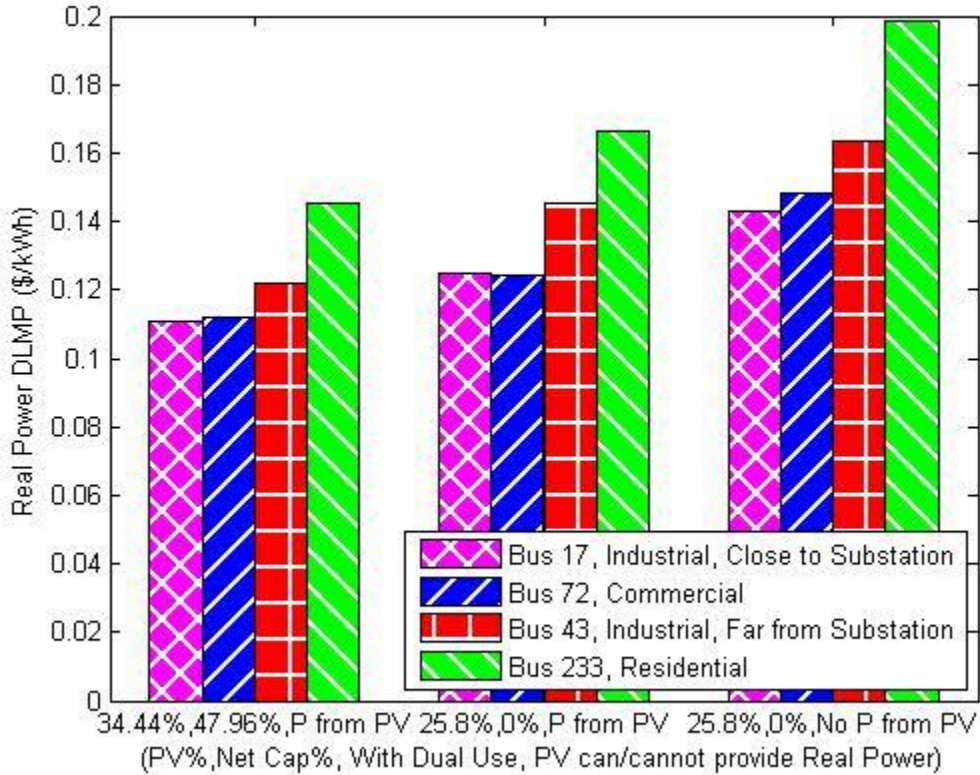
Figure 21. System Peak Hour Real DLMP in the case of No Network Capacitors, with Dual Use of power electronics in PV and EVs.
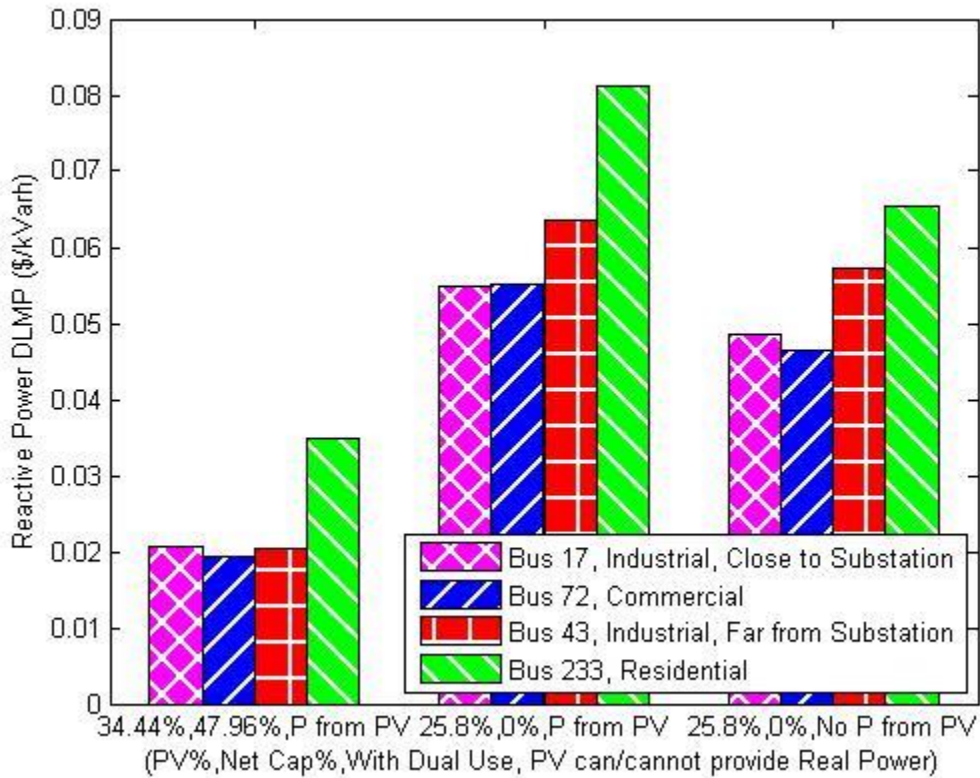

Figure 22. System Peak Hour Reactive DLMP in the case of No Network Capacitors, with Dual Use of power electronics in PV and EVs.
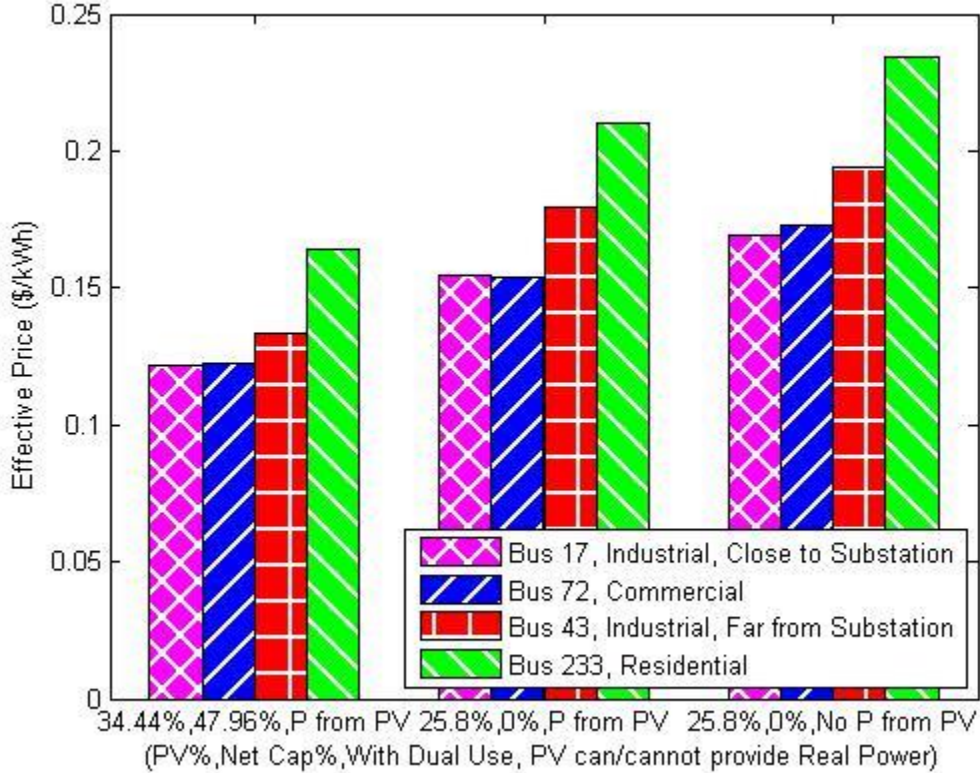
Figure 23. System Peak Hour effective price in the case of No Network Capacitors, with Dual Use of power electronics in PV and EVs.

For the cases where the dual use of power electronics is the only means of reactive power compensation, all of the load is met with only a slight increase in the total and average demand side payments, and while all DLMPs are still of reasonable values. Therefore we can reasonably argue that the case of relying on the dual use of power electronics for reactive power compensation only, is preferable both for the market participants and the Distribution Network Operator.

We focus next on unbundling real and reactive DLMPs as shown in section II.C. Figures 24 and 25 report DLMP components for the system peak hour at busses 17, 72, 43 and 233 when no distributed resources or network capacitors are in use (i.e. the case of Table II and Figures 1-4).
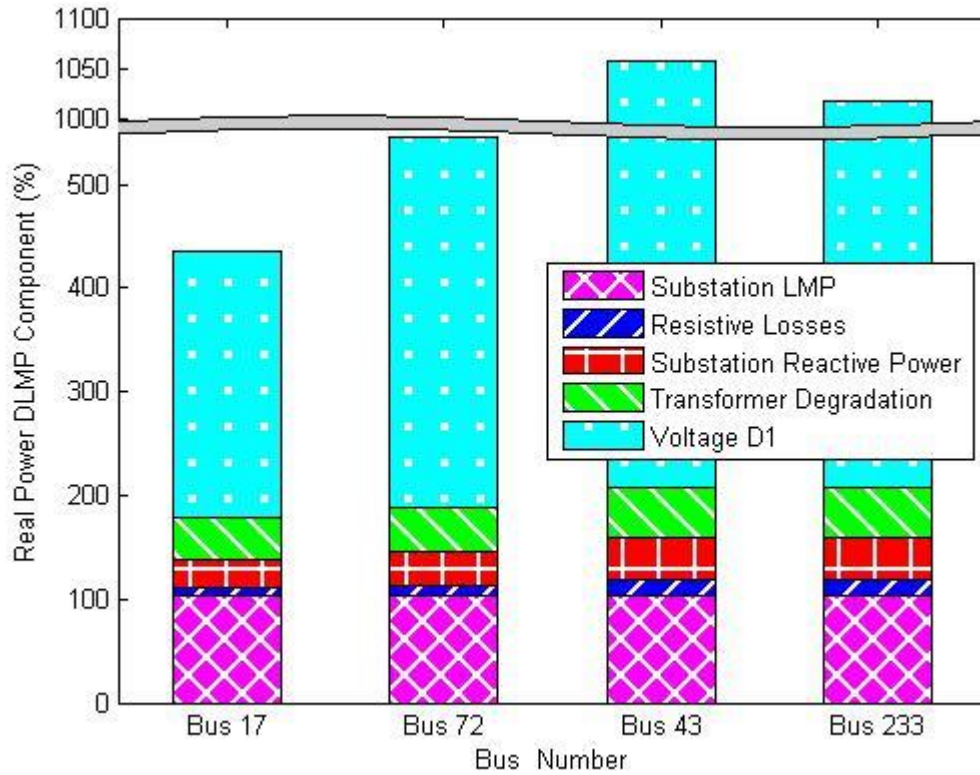
Figure 24. Decomposition of Real Power DLMPs, No DG, No network capacitors, No Dual Use.
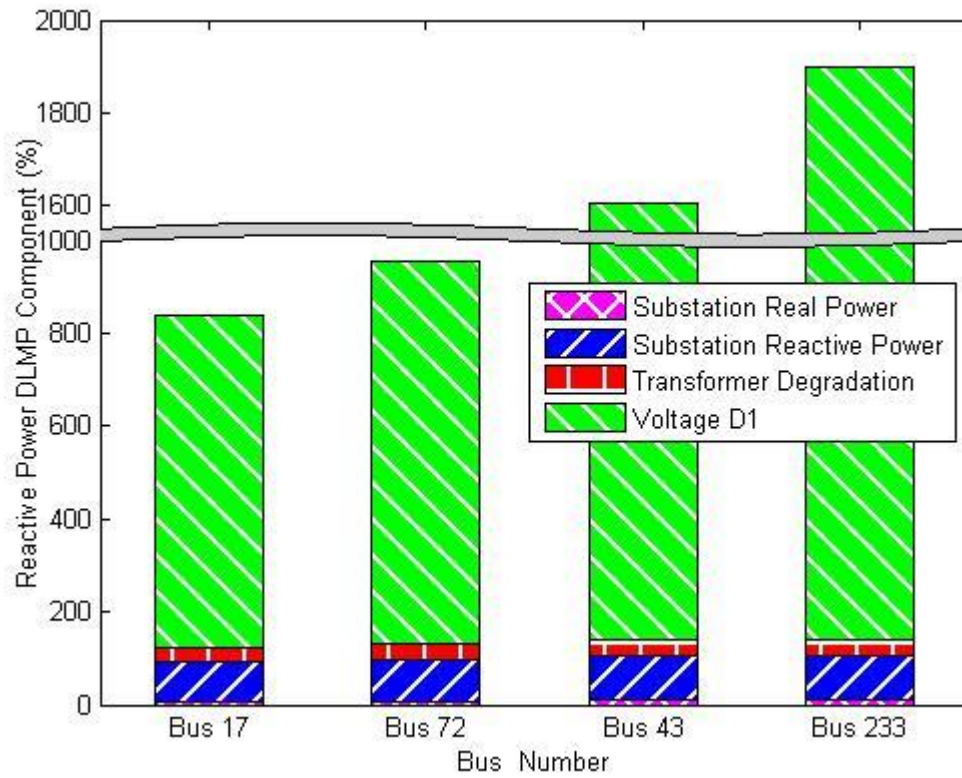
Figure 25. Decomposition of Reactive Power DLMPs, No DG, No network capacitors, No Dual Use.

Figures 26 and 27 below report DLMP components for the system peak hour at busses 17, 72, 43 and 233 when there are no distributed resources nor dual use but only capacitors of total size equal to 47.96% of the total peak reactive demand (Figures 5-7).

Figure 26. Decomposition of Real Power DLMPs, Network Capacitor size 47.96% of total peak reactive demand, No DG, No Dual Use.
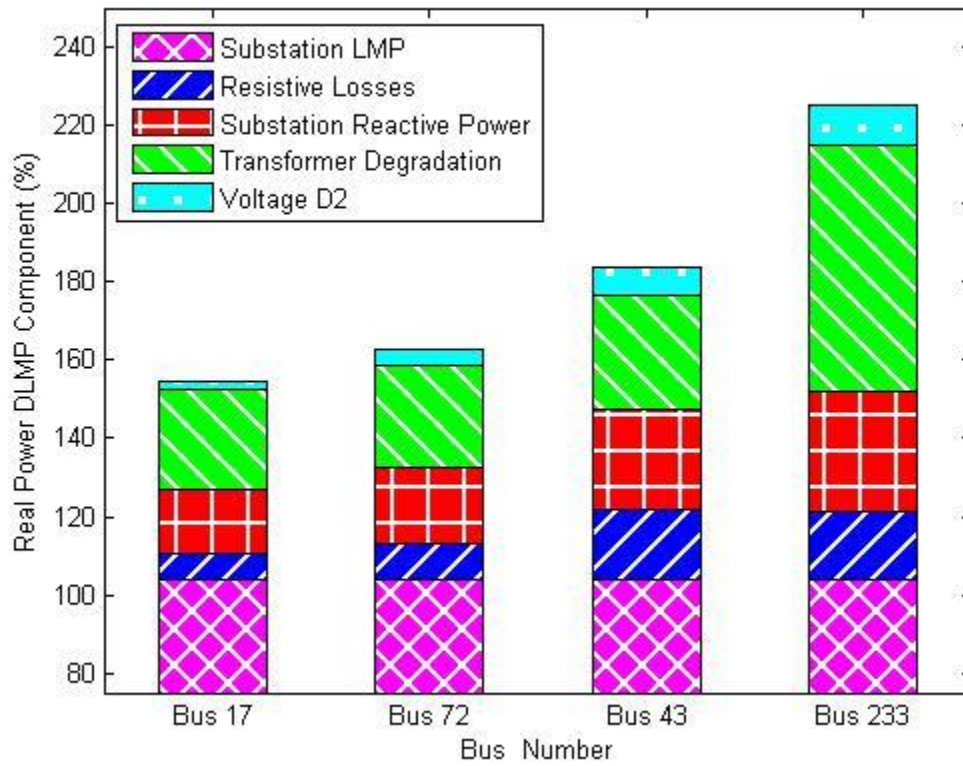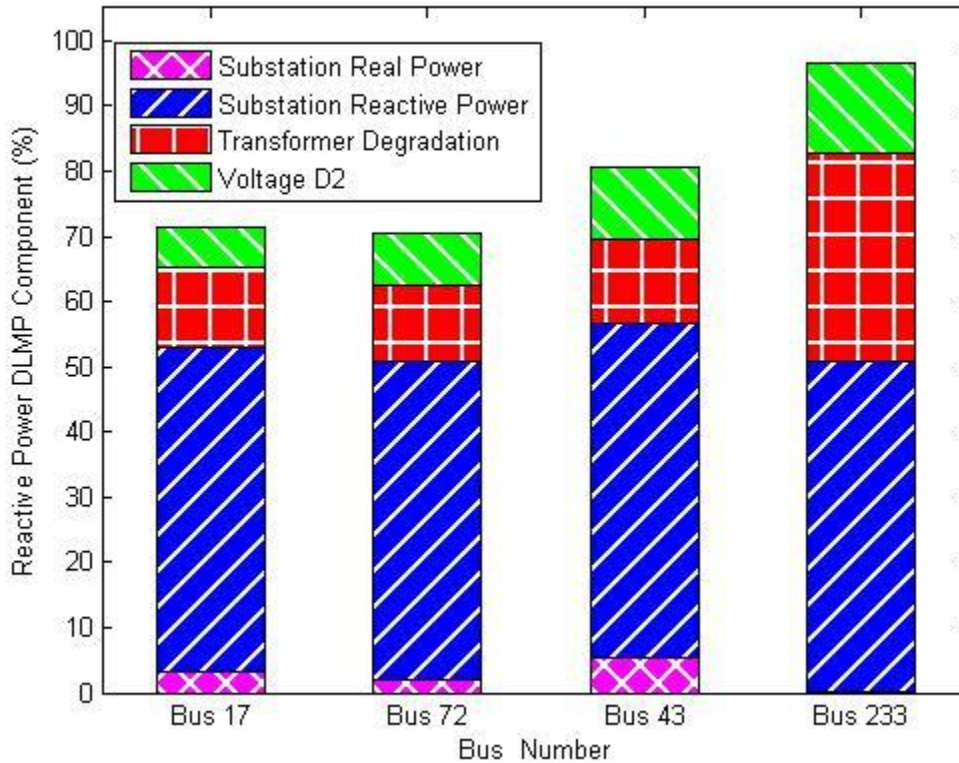
Figure 27. Decomposition of Reactive Power DLMPs, Network Capacitor size 47.96% of total peak reactive demand, No DG, No Dual Use.

For all types of loads, the further a load is from the substation, the larger the losses and the transformer loss of life cost with respect to incremental load. The transformer cost component is much higher in both real and reactive DLMPs for the residential busses. Since additional medium to low voltage transformers are involved this is expected [23].

IV. CONCLUSIONS AND FUTURE WORK

We have investigated the value of real and reactive power provision on distribution networks represented by DLMPs. We show the positive impact of reactive power pricing and conclude that dual use of power electronics for the provision of sufficient reactive power is essential to achieve distribution network resilience to increasing demand. Future work should address modeling of new distribution network assets such as solid state transformers and distribution outage reliability, as well as coupling transmission and distribution in models more accurate than those in [18].

V. REFERENCES

[1] W. Vickrey, "Responsive Pricing of Public Utility Services", Bell Journal of Economics and Management Science, V 2, N 1, 1971.
[2] M. C. Caramanis, R.E. Bohn and F.C Schweppe, "Spot Pricing of Electricity: Practice and theory", IEEE Trans on PAS, V 101, N 9, 1982.
[3] F. C. Schweppe, M. C. Caramanis, R.D. Tabors and R. E. Bohn, Spot Pricing of Electricity, Kluwer, 1987.
[4] A.L. Ott, "Experience with PJM Market Operation, System Design, and Implementation", IEEE Transactions on Power Systems, V 18, N 2, 2003.
[5] www.pnnl.gov
[6] M. Farivar, C. Clarkey, S. Low, M. Chandy, "Inverter VAR Control for Distribution Systems with Renewables", 2011 IEEE International Conference on Smart Grid Communication, pp. 457- 462.
[7] J. Lavaei, S. Low, "Zero Duality Gap In Optimal Power Flow Problem", IEEE Trans on Power Systems, Vol.27, No. 1, February 2012.
[8] H. Chiang, M. E. Baran, "On the existence and uniqueness of load flow solution for radial distribution networks", IEEE Transactions on Circuits and Systems, Volume 37- No.3, March 1990.
[9] "IEEE guide for loading mineral oil immersed transformers", June 14, 1995, pp. 6-7, 14-18, 26-27.
[10] C. Lee, H. Chang, H. Chen, "A method for estimating transformer temperatures and elapsed lives considering operation loads", WSEAS Transactions On Systems, Issue 11, Vol. 7, pp.1349-1358, November 2008.
[11] S. Mohammad, H. Nabavi et al, "Using tracing method for calculation and allocation of reactive power cost", International Journal of Computer Applications, Volume 13- No.2, January 2011.
[12] M. Sasson, FERC Technical Conf on Reactive Power, March 8, 2005.
[13] A.A. El-Keib, X. Ma, "Calculating Short-Run Marginal Costs of Active and Reactive Power Production", IEEE Transactions on Power Systems, Vol. 12, No. 2, May 1997.
[14] H. Liu, L. Tesfatsion, A. A. Chowdhury, "Derivation of locational marginal prices for restructured wholesale power markets", The Journal of Energy Markets (3–27), Volume 2/Number 1, Spring 2009.

[15] M. C. Caramanis, E. Goldis, P. A. Ruiz, A. Rudkevich, "Power Market Reform In the Presence of Flexible Schedulable Distributed Loads. New Bid Rules, Equilibrium and Tractability Issues.", 50th Allerton Conference on Communication, Control and Computing, October 1 - 5, 2012, University of Illinois at Urbana-Champaign, IL, USA.

[16] M. Kraning, E. Chu, J. Lavaei, and S. Boyd, "Dynamic Network Energy Management via Proximal Message Passing", Foundation and Trends In Optimization, Vol 1, No 2, 2013, pp. 70-122.

[17] A. D. Dominguez-Garcia, S. T. Cady, C. N. Hadjicostis, "Decentralized optimal dispatch of distributed energy resources", 2012 IEEE 51st Annual Conference on Decision and Control, pp.3688-3693.

[18] J. Warrington, P. Goulart, S. Mariethoz, M. Morari, "A market mechanism for solving multi-period optimal power flow exactly on AC networks with mixed participants", American Control Conference 2012, June 27-June 29, 2012.

[19] J. Lavaei, S. Sojoudi, "Competitive Equilibria in Electricity Markets with Nonlinearities" American Control Conf 2012, June 27-June 29, 2012. Sathyanarayana, Heydt, "Sensitivity-based pricing and optimal storage utilization in distribution systems," IEEE Transactions on Power Delivery, Vol. 28, No. 2, April 2013.

[20] Sathyanarayana, Heydt, "Sensitivity-based pricing and optimal storage utilization in distribution systems," IEEE Transactions on Power Delivery, Vol. 28, No. 2, April 2013.

[21] N. Steffan, G. T. Heydt, "Quadratic programming and related techniques for the calculation of locational marginal prices in power distribution systems," Proceedings of North American Power Symposium, Champaign IL, September 2012.

[23] R. Li, Q. Wu, S. S. Oren," Distribution Locational Marginal Pricing for Optimal Electric Vehicle Charging Management, IEEE Transactions on Power Systems, to be published.

[23] R.A.Verzijlbergh, Z.Lukszo, J.G.Slootweg, M.D.Ilic, "The impact of controlled electric vehicle charging on residential low voltage networks", 2011 International Conference on Networking, Sensing and Control.

[24] J. Wang, "A planning scheme for penetrating embedded generation in power distribution grids", PhD dissertation, M.I.T., September 2013.

[25] E.Ntakou, M. Caramanis, "Price Discovery in Dynamic Power Markets with Low-Voltage Distribution-Network Participants", Proceedings of the 50th IEEE Transmission & Distribution Conference and Exposition, pp. 1-5.

[26] E. Ntakou, M. Caramanis, "Distribution Network Electricity Market Clearing: Parallelized PMP algorithms with Minimal Coordination", Proceedings of the 53rd IEEE Conference on Decision and Control, December 2014.

[27] www.bu.edu/pcms/caramanis/ElliDistr.pdf

Figure 30. Network topology with busses of interest pointed out.
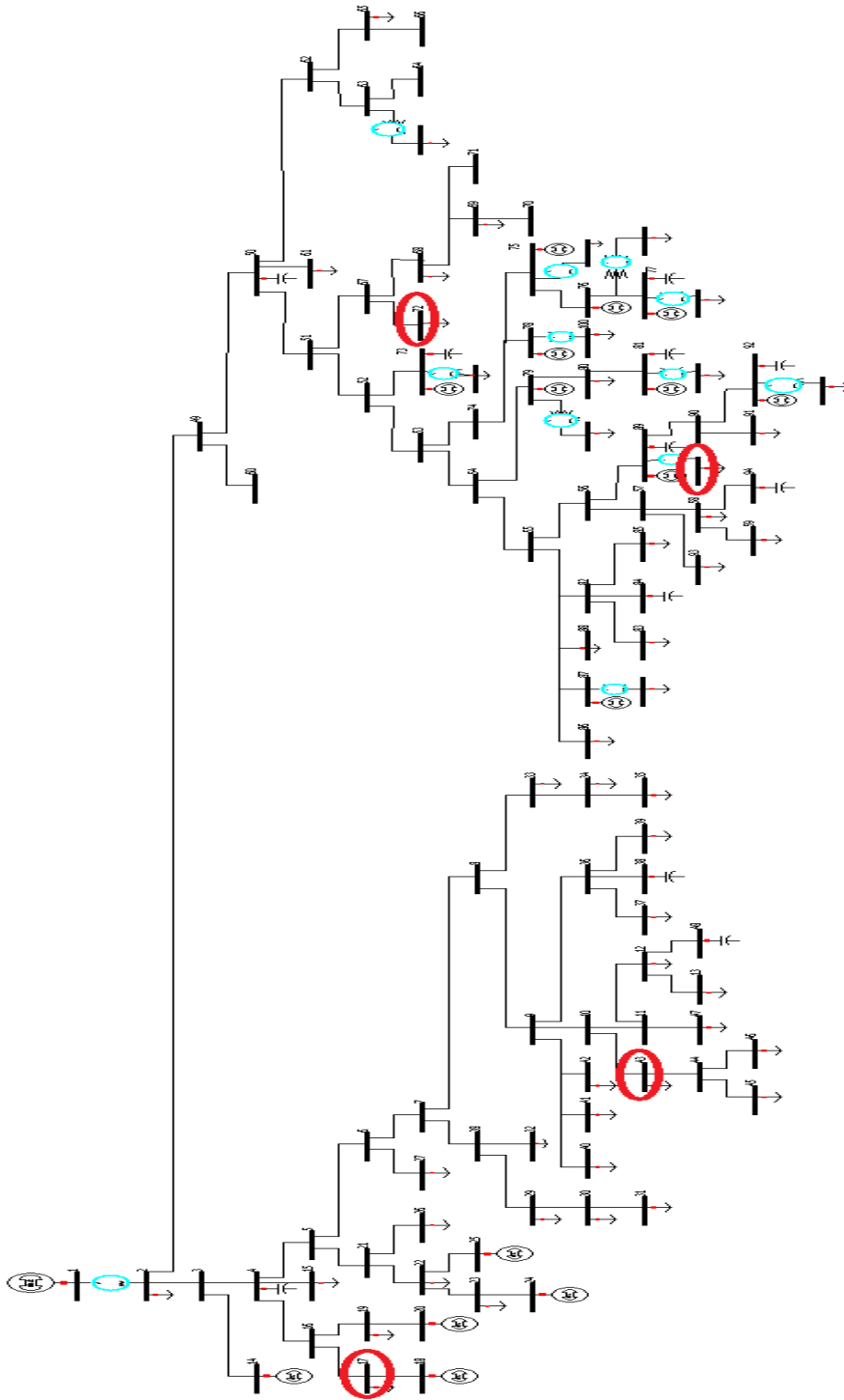
APPENDIX B1. PEAK DEMAND, YEAR 2000.

Bus	Peak Hour Real Demand (MW)	Bus	Peak Hour Real Demand (MW)
2	10.736	42	0.359656
12	0.359656	43	0.069784
13	0.24156	45	0.24156
15	0.477752	46	0.10736
17	0.037576	47	0.24156
19	0.359656	58	0.359656
22	0.24156	59	0.24156
23	1.197064	61	0.477752
26	0.24156	65	0.359656
27	0.10736	68	0.24156
29	0.069784	69	1.197064
30	0.069784	72	0.24156
31	0.10736	80	0.144936
32	0.037576	83	0.144936
33	0.069784	85	0.24156
34	0.144936	86	0.719312
35	0.10736	88	0.359656
37	0.144936	91	0.24156
39	0.24156	93	0.24156
40	0.719312	95-253	0.005368
41	0.069784		

TABLE III. Peak Hour Real Demand Values for the case of fixed loads.

APPENDIX B2. PEAK DEMAND, YEAR 2015.

Bus	Peak Hour Real Demand (MW)	Bus	Peak Hour Real Demand (MW)
2	17.6	42	0.5896
12	0.5896	43	0.1144
13	0.396	45	0.396
15	0.7832	46	0.176
17	0.0616	47	0.396
19	0.5896	58	0.5896
22	0.396	59	0.396
23	1.9624	61	0.7832
26	0.396	65	0.5896
27	0.176	68	0.396
29	0.1144	69	1.9624
30	0.1144	72	0.396
31	0.176	80	0.2376
32	0.0616	83	0.2376
33	0.1144	85	0.396
34	0.2376	86	1.1792
35	0.176	88	0.5896
37	0.2376	91	0.396
39	0.396	93	0.396
40	1.1792	95-253	0.0088
41	0.1144		

TABLE IV. Increased Peak Hour Real Demand Values.

APPENDIX C. SUBSTATION LMP, DEMAND & PV REAL OUTPUT PROFILES

Hour	Substation LMP	Demand Profiles			PV real output profile (% of max Capacity)
		Industrial	Commercial	Residential	
1	76.47	1	0.4	0.5	0.6
2	84.73	1	0.6	0.55	0.8
3	90.97	1	0.8	0.611	1
4	96.37	1	1	0.66	1
5	100.7	1	1	0.722	1
6	103.91	1	1	0.77	1
7	106.1	1	0.8	0.833	1
8	106.57	1	0.6	0.88	0.8
9	106.47	0.8	0.4	0.944	0.4
10	93.16	0.8	0.1	1	0.2
11	81.41	0.8	0.1	0.944	0.2
12	94.52	0.8	0.1	0.88	0
13	75.83	0.8	0.1	0.8	0
14	64.92	0.8	0.1	0.711	0
15	64.95	0.8	0.1	0.622	0
16	67.28	0.8	0.1	0.533	0
17	59.86	0.2	0.1	0.44	0
18	46.79	0.2	0.1	0.55	0
19	42.7	0.2	0.1	0.537	0
20	44.6	0.2	0.1	0.5185	0
21	55.9	0.2	0.1	0.5	0
22	67.84	0.2	0.1	0.48148	0.2
23	69.62	0.2	0.1	0.463	0.2
24	70.35	0.2	0.2	0.4	0.4

TABLE V. Hourly percentage of the peak values for industrial and residential loads and real output of PVs.

APPENDIX D. DISTRIBUTION NETWORK INFORMATION

Capacitors		Photovoltaics	
Bus	**Capacity (MVAr)**	**Bus**	**Capacity (MW)**
4	1.2	**14**	1.5
38	1.8	**18**	0.4
48	1.8	**20**	1.5
50	1.2	**24**	1
84	1.8	**25**	2
94	1.8	**73**	0.64
73	0.756	**75**	0.64
77	0.756	**76**	0.64
81	0.756	**77**	0.64
89	0.756	**78**	0.64
92	0.756	**79**	0.64
		81	0.64
		87	0.64
		89	0.64
		92	0.64

TABLE VI. Location and Nameplate Capacity of Photovoltaics and Capacitors.

Transformer Characteristics	High to Medium Voltage	Medium to Low Voltage
Nameplate Capacity (kVA)	30000	75, 100 or 150
Location in network (bus from-bus to)	1-2	63-95, 73-102, 75-122, 76-135, 77-148, 78-168, 79-175, 81-188, 87-208, 89-221, 92-234
Total lifetime	20 years	10 years

TABLE VII. Transformer Characteristics.

APPENDIX E. ELECTRIC VEHICLE INPUTS

Electric Vehicles	EV connection bus	Battery Charging Demand (kWh)	EV charging rate (kW)	EV power electronics capacity (kVA)	Arrival Time		Departure Time	
Industrial Feeder	23, 40	24	6.6	44	**1st class**	9am	**1st class**	5pm
					2nd class	5pm	**2nd class**	1am
Commercial Sub-feeder	58, 59, 61, 65, 68, 69, 72, 80, 83, 85, 86, 88, 91, 93	24	6.6	44	9am		5pm	
Residential Sub-feeders	95, 102, 122, 135, 148, 168, 175, 188, 208, 221, 234	24	3.3	44	6pm		8am	

TABLE VIII. Electric Vehicles characteristics